

Effect of the particle-hole channel on BCS–Bose-Einstein condensation crossover in atomic Fermi gases

Qijin Chen

Department of Physics and Zhejiang Institute of Modern Physics,
Zhejiang University, Hangzhou, Zhejiang 310027, CHINA
(Dated: February 24, 2012)

BCS–Bose-Einstein condensation (BEC) crossover is effected by increasing pairing strength between fermions from weak to strong in the particle-particle channel. Here we study the effect of the particle-hole channel on the zero T gap $\Delta(0)$, superfluid transition temperature T_c and the pseudogap at T_c , as well as the mean-field ratio $2\Delta(0)/T_c^{\text{MF}}$, from BCS through BEC regimes, in the framework of a pairing fluctuation theory which includes self-consistently the contributions of finite-momentum pairs. These pairs necessarily lead to a pseudogap in single particle excitation spectrum above and below T_c . We sum over the infinite particle-hole ladder diagrams so that the particle-particle and particle-hole T -matrices are entangled with each other. We find that the particle-hole susceptibility has a complex dynamical structure, with strong momentum and frequency dependencies, and is sensitive to temperature, gap size and interaction strength. We conclude that neglecting the self-energy feedback causes a serious over-estimate of the particle-hole susceptibility. In the BCS limit, the particle-hole channel effect may be approximated by the same reduction in the overall pairing strength so that the ratio $2\Delta(0)/T_c$ is unaffected, in agreement with Gor'kov *et al.* to the leading order. However, the effect becomes more complex and pronounced in the crossover regime, where the particle-hole susceptibility is reduced by both a smaller Fermi surface and a big (pseudo)gap. Deep in the BEC regime, the particle-hole channel contributions drop to zero. We propose that precision measurements of the magnetic field for Feshbach resonance at low temperatures as a function of density can be used to quantify the particle-hole susceptibility and test different theories.

PACS numbers: 03.75.Ss, 03.75.Nt, 74.20.-z, 74.25.Dw

I. INTRODUCTION

BCS–Bose-Einstein condensation (BEC) crossover has been an interesting research subject since 1980's [1–29]. The experimental realization of BCS-BEC crossover in ultracold atomic Fermi gases [30–39], with the help of Feshbach resonances, has given it a strong boost [40–59] over the past several years. When the pairing interaction is tuned from weak to strong in a two component Fermi gas, the superfluid behavior evolves continuously from the type of BCS to that of BEC [2, 3, 29].

In such a fundamentally fermionic system, superfluidity mainly concerns pairing, namely, interactions in the particle-particle channel. In contrast, the particle-hole channel mainly causes a chemical potential shift, and is often neglected [60]. For example, in a conventional superconductor, the chemical potential below and above T_c are essentially the same, and thus its dependence on the temperature and the interaction strength has been completely neglected in the weak coupling BCS theory for normal metal superconductors. On the other hand, Gor'kov and Melik-Barkhudarov (GMB) [61] considered the lowest order correction from the particle-hole channel, (which has been referred to as induced interaction in the literature), and found that both T_c and zero temperature gap $\Delta(0)$ are suppressed by a *big* factor of $(4e)^{1/3} \approx 2.22$. Berk and Schrieffer [62] also studied a similar effect in the form of ferromagnetic spin correlations in superconductors. Despite the big size of the GMB correction, the effect of the particle-hole channel has been largely overlooked in the theoretical study of BCS-BEC crossover, until it has become realistic to achieve such crossover experimentally in atomic Fermi

gases. Heiselberg and coworkers [63] considered the effect of the lowest order induced interaction in dilute Fermi gases and generalized it to the case of multispecies of fermions as well as the possibility of exchange of bosons. Kim *et al.* [64] considered the lowest order induced interactions in optical lattices. Within the *mean-field* treatment and *without* including the excitation gap in the particle and hole propagators, these authors found the same effective overall interaction at zero T and at T_c and hence an unaffected mean-field ratio $2\Delta(0)/k_B T_c \approx 3.53$. Martikainen *et al.* [65] considered the lowest order induced interactions in a three-component Fermi gas. It has become clear that including only the perturbative lowest order induced interaction is *not* appropriate away from the weak coupling BCS regime. Yin and coworkers [66] went beyond the lowest order and considered the induced interactions from all particle-hole ladder diagrams, i.e., the entire particle-hole T -matrix. However, in all the above works, only the *bare* particle-hole susceptibility χ_{ph}^0 was considered, and it was averaged on-shell and only on the Fermi surface, with equal momenta for the particle and the hole propagators. No self-energy feedback was included. Therefore, there was necessarily no pseudogap in the fermion excitation spectrum at T_c . This is basically equivalent to replacing the particle-hole susceptibility χ_{ph}^0 by an essentially temperature independent constant, leading to a simple downshift in the pairing interaction.

As the gap and T_c increase with interaction strength, it can naturally be expected that the contribution from the particle-hole channel, or the induced interaction, will acquire a significant temperature dependence. More importantly, *the presence of the (pseudo)gap serves to suppress the particle-hole fluctu-*

ations (which tend to break pairing). In other words, neglecting the feedback of the gap related self energy in the particle-hole susceptibility is expected to cause an over-estimate of the particle-hole channel contributions. Therefore, a proper treatment should include the gap effect in the particle-hole susceptibility. In addition, the lowest order treatment is no longer appropriate away from the weak coupling regime.

Furthermore, it has now been established that as the pairing interaction increases, pseudogap develops naturally [29, 67]. Experimental evidence for its existence comes from high T_c superconductors [29, 68–70] as well as atomic Fermi gases [71–75]. Therefore, a theory with proper treatment of the pseudogap effect is necessary in order to arrive at results that can be *quantitatively* compared with experiment. For the same reason, the effect of the particle-hole channel needs also to be studied within such a theory.

In this paper, we explore the particle-hole channel effect based on a pairing fluctuation theory [21, 22], originally developed for treating the pseudogap phenomena of high T_c superconductors. This theory has been successfully applied to atomic Fermi gases and has been generating results that are in good agreement with experiment [29, 71, 73]. Here we include the entire particle-hole T -matrix, with gap effect included in the fermion Green's functions. Instead of a simple average of the particle-hole susceptibility χ_{ph} on the Fermi surface, here we choose to average at two different levels – one on the Fermi surface, one over a narrow momentum shell around the Fermi level. We find that χ_{ph} has very strong frequency and momentum as well as temperature dependencies. It is sensitive to the gap size. Therefore, self-consistently including the self-energy feedback is important. For both levels of average, we find that while in the BCS limit, the particle-hole channel effect may be approximated by a downshift in the pairing strength so that the ratio $2\Delta(0)/T_c$ is unaffected, the situation becomes more complex as the interaction becomes stronger where the gap is no longer very small. Significant difference exists for these two levels of averaging. The particle-hole susceptibility is reduced by both a smaller Fermi surface and a big (pseudo)gap in the crossover regime. Deep in the BEC regime, the particle-hole channel contributions drop to zero. Without including the incoherent part of the self energy, we find that at unitarity, $T_c/E_F \approx 0.217$, in reasonable agreement with experiment.

The rest of this paper is arranged as follows. In Sec. II, we first give a brief summary of the pairing fluctuation theory without the particle-hole channel effect. Then we derive the theory with particle-hole channel included, starting by studying the dynamic structure of the particle-hole susceptibility. Next, in Sec. III, we present numerical results, showing the effect of the particle-hole channel on the zero T gap, transition temperature T_c and pseudogap at T_c , as well as the mean-field ratio $2\Delta(0)/T_c^{MF}$. We also discuss and compare our value of T_c/E_F with experiment and those in the literature. Finally, we conclude in Sec. IV. More detailed results on the dynamic structure of the particle-hole susceptibility are presented in the Appendix.

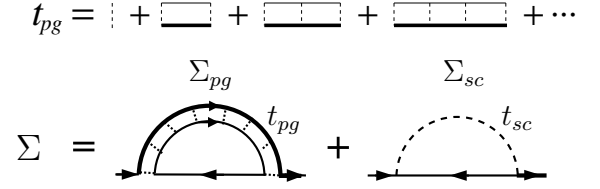


Figure 1. Feynman diagrams for the particle-particle channel T -matrix t_{pg} and the self energy $\Sigma(K)$. The dotted lines represent the bare pairing interaction U . The dashed line, t_{sc} , represents the superfluid condensate.

II. PAIRING FLUCTUATION THEORY WITH THE PARTICLE-HOLE CHANNEL EFFECT INCLUDED

A. Summary of the pairing fluctuation theory without the particle-hole channel effect

To make this paper self-contained and to introduce the assumptions as well as the notations, we start by summarizing the pairing fluctuation theory [21, 22] without the effect of the particle-hole channel, as a foundation for adding the particle-hole channel.

We consider a Fermi gas with a short range s -wave interaction $U(\mathbf{k}, \mathbf{k}') = U < 0$, which exists only between opposite spins. Our theory can be effectively represented by a T -matrix approximation, shown diagrammatically in Fig. 1. However, we emphasize that this is *not* a diagrammatic approach, since Fig. 1 is simply a representation of the equations derived from an equation of motion approach [22, 76–78]. The self energy $\Sigma(K)$ comes from two contributions, associated with the superfluid condensate and finite momentum pairs, respectively, given by $\Sigma(K) = \Sigma_{sc}(K) + \Sigma_{pg}(K)$, where

$$\Sigma_{sc}(K) = \frac{\Delta_{sc}^2}{i\omega_l + \xi_{\mathbf{k}}}, \quad \Sigma_{pg}(K) = \sum_Q t_{pg}(Q) G_0(Q - K), \quad (1)$$

with Δ_{sc} being the superfluid order parameter. We use a four-vector notation, $K \equiv (\mathbf{k}, i\omega_l)$, $Q \equiv (\mathbf{q}, i\Omega_n)$, $\sum_K \equiv T \sum_{l, \mathbf{k}}$, etc., and ω_l and Ω_n are odd and even Matsubara frequencies for fermions and bosons, respectively. Here $G_0(K) = (i\omega_l - \xi_{\mathbf{k}})^{-1}$ and $G(K) = [G_0^{-1} - \Sigma(K)]^{-1}$ are the bare and full Green's functions, respectively, $\xi_{\mathbf{k}} = \hbar^2 k^2 / 2m - \mu$ is the free fermion dispersion, measured with respect to the Fermi level. In what follows, we will set $k_B = \hbar = 1$. The pseudogap T -matrix

$$t_{pg}(Q) = \frac{U}{1 + U\chi(Q)} \quad (2)$$

can be regarded as the renormalized pairing interaction with pair momentum Q , where

$$\chi(Q) = \sum_K G(K) G_0(Q - K) \quad (3)$$

is the pair susceptibility. We emphasize that this asymmetric form of $\chi(Q)$ is not an *ad hoc* choice but rather a natural re-

sult of the equation of motion method. The bare Green's function G_0 comes from the inversion of the operator G_0^{-1} which appears on the left hand side of the equations of motion. It also appears in the particle-hole susceptibility χ_{ph} , as will be shown below. Albeit not a phi-derivable theory, the equation of motion method ensures that this theory is more consistent with the Hamiltonian than a phi-derivable theory.

The gap equation is given by the pairing instability condition,

$$1 + U\chi(0) = 0, \quad (T \leq T_c), \quad (4)$$

referred to as the Thouless criterion, which can also be naturally interpreted as the Bose condensation condition for the pairs, since $1 + U\chi(0) \propto \mu_{\text{pair}}$. In fact, after analytical continuation $i\Omega_n \rightarrow \Omega + i0^+$, one can Taylor expand the (inverse) T -matrix as

$$t_{pg}(\Omega, \mathbf{q}) \approx \frac{Z^{-1}}{\Omega - \Omega_{\mathbf{q}} + \mu_{\text{pair}} + i\Gamma_{\mathbf{q}}}, \quad (5)$$

and thus extract the pair dispersion $\Omega_{\mathbf{q}} \approx q^2/2M^*$ to the leading order, where M^* is the effective pair mass. Here $\Gamma_{\mathbf{q}}$ is the imaginary part of the pair dispersion and can be neglected when pairs become (meta)stable [21, 22, 78]. In the superfluid phase, $t_{pg}(Q)$ diverges at $Q = 0$ and a macroscopic occupation of the $Q = 0$ Cooper pairs, i.e., the condensate, appears. This macroscopic occupation, has to be expressed as a singular term, $t_{sc}(Q) = -(\Delta_{sc}^2/T)\delta(Q)$, (the dashed line in Fig. 1), such that $\Sigma_{sc}(K) = \sum_Q t_{sc}(Q)G_0(Q - K)$, written in the same form as its pseudogap counterpart, $\Sigma_{pg}(K)$.

Now we split $\Sigma_{pg}(K)$ into coherent and incoherent parts:

$$\begin{aligned} \Sigma_{pg}(K) &= \sum_Q \frac{t_{pg}(Q)}{i\Omega_n - i\omega_l - \xi_{\mathbf{q}-\mathbf{k}}} \\ &= -\sum_Q \frac{t_{pg}(Q)}{i\omega_l + \xi_{\mathbf{k}}} + \delta\Sigma = \frac{\Delta_{pg}^2}{i\omega_l + \xi_{\mathbf{k}}} + \delta\Sigma, \end{aligned} \quad (6)$$

where we have defined the pseudogap Δ_{pg} via

$$\Delta_{pg}^2 \equiv -\sum_Q t_{pg}(Q) \approx Z^{-1} \sum_{\mathbf{q}} b(\Omega_{\mathbf{q}}), \quad (7)$$

where $b(x)$ is the Bose distribution function. Below T_c , the divergence of $t_{pg}(Q = 0)$ makes it a good mathematical approximation to neglect the incoherent term $\delta\Sigma$ so that

$$\Sigma(K) \approx \frac{\Delta^2}{i\omega_l + \xi_{\mathbf{k}}}, \quad \text{with} \quad \Delta^2 = \Delta_{sc}^2 + \Delta_{pg}^2. \quad (8)$$

Therefore, the Green's function $G(K)$, the quasiparticle dispersion $E_{\mathbf{k}} = \sqrt{\xi_{\mathbf{k}}^2 + \Delta^2}$, and the gap equation, as expanded from Eq. (4), follow the same BCS form, *except that the total gap Δ now contains both contributions from the order parameter Δ_{sc} and the pseudogap Δ_{pg} .*

For a contact potential, we get rid of the interaction U in favor of the scattering length a via $m/4\pi a = 1/U +$

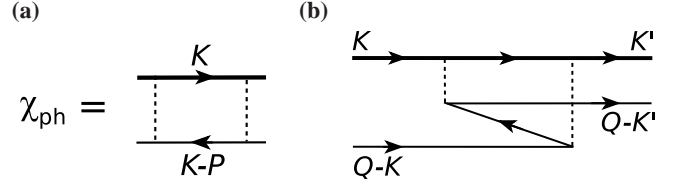


Figure 2. Feynman diagrams for the particle-hole susceptibility χ_{ph} in the presence of self-energy feedback effect. Panel (b) is identical to panel (a), with twisted external legs. The total particle-hole momentum P in (a) is equal to $K + K' - Q$ in (b), with Q being the particle-particle pair momentum.

$\sum_{\mathbf{k}} (1/2\epsilon_{\mathbf{k}})$, where $\epsilon_{\mathbf{k}} = k^2/2m$. Then the gap equation can be written as

$$-\frac{m}{4\pi a} = \sum_{\mathbf{k}} \left[\frac{1 - 2f(E_{\mathbf{k}})}{2E_{\mathbf{k}}} - \frac{1}{2\epsilon_{\mathbf{k}}} \right], \quad (9)$$

where $f(x)$ is the Fermi distribution function. In addition, we have the particle number constraint, $n = 2 \sum_{\mathbf{K}} G(K)$, i.e.,

$$n = 2 \sum_{\mathbf{k}} \left[v_{\mathbf{k}}^2 + \frac{\xi_{\mathbf{k}}}{E_{\mathbf{k}}} f(E_{\mathbf{k}}) \right], \quad (10)$$

where $v_{\mathbf{k}}^2 = (1 - \xi_{\mathbf{k}}/E_{\mathbf{k}})/2$ is the BCS coherence factor.

Equations (9), (10), and (7) form a closed set. For given interaction $1/k_F a$, they can be used to solve self consistently for T_c as well as Δ and μ at T_c , or for Δ , Δ_{sc} , Δ_{pg} , and μ as a function of T below T_c . Here k_F is the Fermi wave vector. More details about the Taylor expansion of the inverse T matrix can be found in Refs. [78, 79].

B. Dynamic structure of particle-hole susceptibility $\chi_{ph}(P)$

Before we derive the theory with full particle-hole T -matrix t_{ph} included, we first study the dynamic structure of the particle-hole susceptibility $\chi_{ph}(P)$. It is the single rung of the particle-hole scattering ladder diagrams, as shown in Fig. 2(a). Note that direct interaction exists only between fermions of opposite spins. Therefore, the particle and hole must also have opposite spins. The total particle-hole four-momentum is given by $P \equiv (i\nu_n, \mathbf{p})$. Since we are considering the effect on pairing induced by the particle-hole channel, we can twist external legs of the diagram, as shown in Fig. 2(b), so that the particle-hole contribution can be added to the original pairing interaction U directly. It is obvious that the particle-hole momentum P in Fig. 2(a) are equal to $K + K' - Q$ in Fig. 2(b), where Q is the pair momentum of the particle-particle channel. Therefore, we have

$$\begin{aligned} \chi_{ph}(P) &= \sum_K G(K)G_0(K - P) \\ &= \sum_{\mathbf{k}} \left[\frac{f(E_{\mathbf{k}}) - f(\xi_{\mathbf{k}-\mathbf{p}})}{E_{\mathbf{k}} - \xi_{\mathbf{k}-\mathbf{p}} - i\nu_n} u_{\mathbf{k}}^2 - \frac{1 - f(E_{\mathbf{k}}) - f(\xi_{\mathbf{k}-\mathbf{p}})}{E_{\mathbf{k}} + \xi_{\mathbf{k}-\mathbf{p}} + i\nu_n} v_{\mathbf{k}}^2 \right]. \end{aligned} \quad (11)$$

Note that again we have a mixing of dressed and undressed Green's function in $\chi_{\text{ph}}(P)$, like in the expression of $\chi(Q)$. As mentioned earlier, this mixing has exactly the same origin in both cases [80]. For convenience, here we dress the particle propagator with self energy and leave the hole propagator undressed. This is based on the fact that the hole propagator is undressed in $\chi(Q)$ in Sec. II A. (One can equivalently dress the hole while leaving the particle undressed).

A few remarks are in order. Firstly, in the center-of-mass (COM) reference frame of a particle-particle pair, the momenta in Fig. 2(b) will be relabeled as $\pm K + Q/2$ and $\pm K' + Q/2$, so that $P = (K + Q/2) - (-K' + Q/2) = K + K'$, independent of the total pair momentum Q . Here $\pm K$ and $\pm K'$ are the four momenta of the incoming and outgoing fermions in the COM reference frame. Therefore, the induced interactions still conform to the Galileo transformation. Secondly, as in the Nozières and Schmitt-Rink (NSR) theory [3], one needs a fictitious separable potential $U_{\mathbf{k},\mathbf{k}'} = U\varphi_{\mathbf{k}}\varphi_{\mathbf{k}'}$ in order to have a simple result in the form of Eq. (2) for the summation of the particle-particle ladder diagrams [17, 21, 22]. The contact potential considered for atomic Fermi gases automatically satisfies this requirement. However, since the particle-hole pair susceptibility $\chi_{\text{ph}}(P)$ only depends on the sum $P = K + K'$, it is obvious that when the particle-hole contribution is included, the total effective interaction $U_{\text{eff}}(\mathbf{k}, \mathbf{k}')$ will no longer be separable. Approximate treatment is needed, as will be shown later.

To proceed, we separate the retarded χ_{ph}^R into real and imaginary parts, $\chi_{\text{ph}}^R(\nu, \mathbf{p}) = \chi'_{\text{ph}}(\nu, \mathbf{p}) + i\chi''_{\text{ph}}(\nu, \mathbf{p})$, after analytical continuation, $i\nu_n \rightarrow \nu + i0^+$. We have

$$\chi'_{\text{ph}}(\nu, \mathbf{p}) = \sum_{\mathbf{k}} \left[\frac{f(E_{\mathbf{k}}) - f(\xi_{\mathbf{k}-\mathbf{p}})}{E_{\mathbf{k}} - \xi_{\mathbf{k}-\mathbf{p}} - \nu} u_{\mathbf{k}}^2 - \frac{1 - f(E_{\mathbf{k}}) - f(\xi_{\mathbf{k}-\mathbf{p}})}{E_{\mathbf{k}} + \xi_{\mathbf{k}-\mathbf{p}} + \nu} v_{\mathbf{k}}^2 \right], \quad (12a)$$

$$\chi''_{\text{ph}}(\nu, \mathbf{p}) = \pi \sum_{\mathbf{k}} \left\{ [f(E_{\mathbf{k}}) - f(E_{\mathbf{k}} - \nu)] u_{\mathbf{k}}^2 \delta(E_{\mathbf{k}} - \xi_{\mathbf{k}-\mathbf{p}} - \nu) + [f(E_{\mathbf{k}} + \nu) - f(E_{\mathbf{k}})] v_{\mathbf{k}}^2 \delta(E_{\mathbf{k}} + \xi_{\mathbf{k}-\mathbf{p}} + \nu) \right\}. \quad (12b)$$

From Eq. (12b), we can immediately conclude $\chi''_{\text{ph}}(0, \mathbf{p}) = 0$. In addition, $\chi''_{\text{ph}}(\nu, 0) = 0$ if $-\min(E_{\mathbf{k}} + \xi_{\mathbf{k}}) = -(\sqrt{\mu^2 + \Delta^2} - \mu) < \nu < 0$ or $\nu > \max(E_{\mathbf{k}} - \xi_{\mathbf{k}}) = \sqrt{\mu^2 + \Delta^2} + \mu$. At low T , we also have $\chi''_{\text{ph}}(\nu, 0)$ exponentially small for $|\nu| < \Delta$ if $\mu > 0$ or for $|\nu| < \sqrt{\mu^2 + \Delta^2}$ otherwise. In all cases, $\chi_{\text{ph}}^R(\nu, \mathbf{p}) = \chi_{\text{ph}}^R(\nu, p)$ is isotropic in \mathbf{p} . In the BCS limit, $\Delta \rightarrow 0$, $E_{\mathbf{k}} \rightarrow |\xi_{\mathbf{k}}|$, so that

$$\chi'_{\text{ph}}(0, p \rightarrow 0) \approx \sum_{\mathbf{k}} f'(\xi_{\mathbf{k}}) = -\frac{mk_{\mu}}{2\pi^2}, \quad (13)$$

where $k_{\mu} = \sqrt{2m\mu}$ is the momentum on the Fermi surface.

For comparison, we also study the dynamic structure of the

undressed particle-hole pair susceptibility,

$$\chi_{\text{ph}}^0(P) = \sum_{\mathbf{K}} G_0(K)G_0(K - P) = \sum_{\mathbf{k}} \frac{f(\xi_{\mathbf{k}}) - f(\xi_{\mathbf{k}-\mathbf{p}})}{\xi_{\mathbf{k}} - \xi_{\mathbf{k}-\mathbf{p}} - i\nu_n}. \quad (14)$$

This is the particle-hole pair susceptibility studied by GMB [61] and others [63–66] in the literature. The imaginary part is given by

$$\chi_{\text{ph}}^{0''}(\nu, \mathbf{p}) = \pi \sum_{\mathbf{k}} [f(\xi_{\mathbf{k}}) - f(\xi_{\mathbf{k}} - \nu)] \delta(\xi_{\mathbf{k}} - \xi_{\mathbf{k}-\mathbf{p}} - \nu). \quad (15)$$

Same as in the $\chi_{\text{ph}}(P)$ case, we have $\chi_{\text{ph}}^{0''}(0, \mathbf{p}) = 0$. For finite $\nu \neq 0$, $\chi_{\text{ph}}^{0''}(\nu, \mathbf{p}) \rightarrow 0$ exponentially as $p \rightarrow 0$. The real part satisfies

$$\chi_{\text{ph}}^{0'}(\nu \neq 0, 0) = 0 \quad (16)$$

and

$$\chi_{\text{ph}}^{0'}(0, p \rightarrow 0) = \sum_{\mathbf{k}} f'(\xi_{\mathbf{k}}) \approx -\frac{mk_{\mu}}{2\pi^2} \quad (17)$$

at low T . More generally, for $\nu = 0$ and finite p , we have

$$\chi_{\text{ph}}^{0'}(0, p) = \int_0^\infty \frac{kd k}{2\pi^2} \frac{m}{p} f(\xi_{\mathbf{k}}) \ln \left| \frac{2k - p}{2k + p} \right|. \quad (18)$$

In the weak coupling limit, $\chi'_{\text{ph}}(0, p \rightarrow 0) = \chi_{\text{ph}}^{0'}(0, p \rightarrow 0)$, since χ_{ph} reduces to χ_{ph}^0 when the gap Δ vanishes.

Let's take a look at the case of *small* but finite p . Equation (15) can be rewritten as

$$\begin{aligned} \chi_{\text{ph}}^{0''}(\nu, \mathbf{p}) &= \pi \sum_{\mathbf{k}} [f(\xi_{\mathbf{k}}) - f(\xi_{\mathbf{k}} - \nu)] \delta \left(\frac{\mathbf{k} \cdot \mathbf{p}}{m} - \frac{p^2}{2m} - \nu \right) \\ &\approx \pi \nu \sum_{\mathbf{k}} f'(\xi_{\mathbf{k}}) \delta \left(\frac{\mathbf{k} \cdot \mathbf{p}}{m} - \frac{p^2}{2m} - \nu \right) \propto \nu. \end{aligned} \quad (19)$$

The delta function can be satisfied only at $k \gtrsim |\nu|m/p$. When $|\nu|m/p > k_{\mu}$, $\xi_{\mathbf{k}} > 0$ for all k so that the magnitude of $\chi_{\text{ph}}^{0''}(\nu, \mathbf{p})$ will also turn around and start to decrease exponentially. The turning points $\nu = \pm p k_{\mu}/m$ show up as two peaks in $\chi_{\text{ph}}^{0'}(\nu, \mathbf{p})$.

It is easy to show that the hermitian conjugate $\chi_{\text{ph}}^{0R*}(\nu, \mathbf{p}) = \chi_{\text{ph}}^{0R}(-\nu, \mathbf{p})$. Similar relations do not hold for χ_{ph} , however, due to the mixing of G_0 and G in the expression of $\chi_{\text{ph}}(P)$.

Shown in Figs. 3(a) and 3(b) are three dimensional (3D) plots of the real and imaginary parts of $\chi_{\text{ph}}^{0R}(\nu, \mathbf{p})$. In Figs. 3(c) through 3(f) we present our calculated results of $\chi_{\text{ph}}^R(\nu, \mathbf{p})$ in the presence of self energy feedback. They are calculated at T_c (a-d) and $0.1T_c$ (e,f) in the unitary limit, $1/k_F a = 0$. Here $T_c/E_F \approx 0.256$ is the one calculated in the pairing fluctuation theory without including the particle-hole channel contribution. The even and odd symmetries of $\chi_{\text{ph}}^{0'}(\nu, \mathbf{p})$ and $\chi_{\text{ph}}^{0''}(\nu, \mathbf{p})$ with respect to $\nu \rightarrow -\nu$ are evident. And indeed these symmetries are not present for $\chi_{\text{ph}}^R(\nu, \mathbf{p})$. The interesting structure at low frequency and low momentum clearly derives from the pseudogap already present at T_c in the

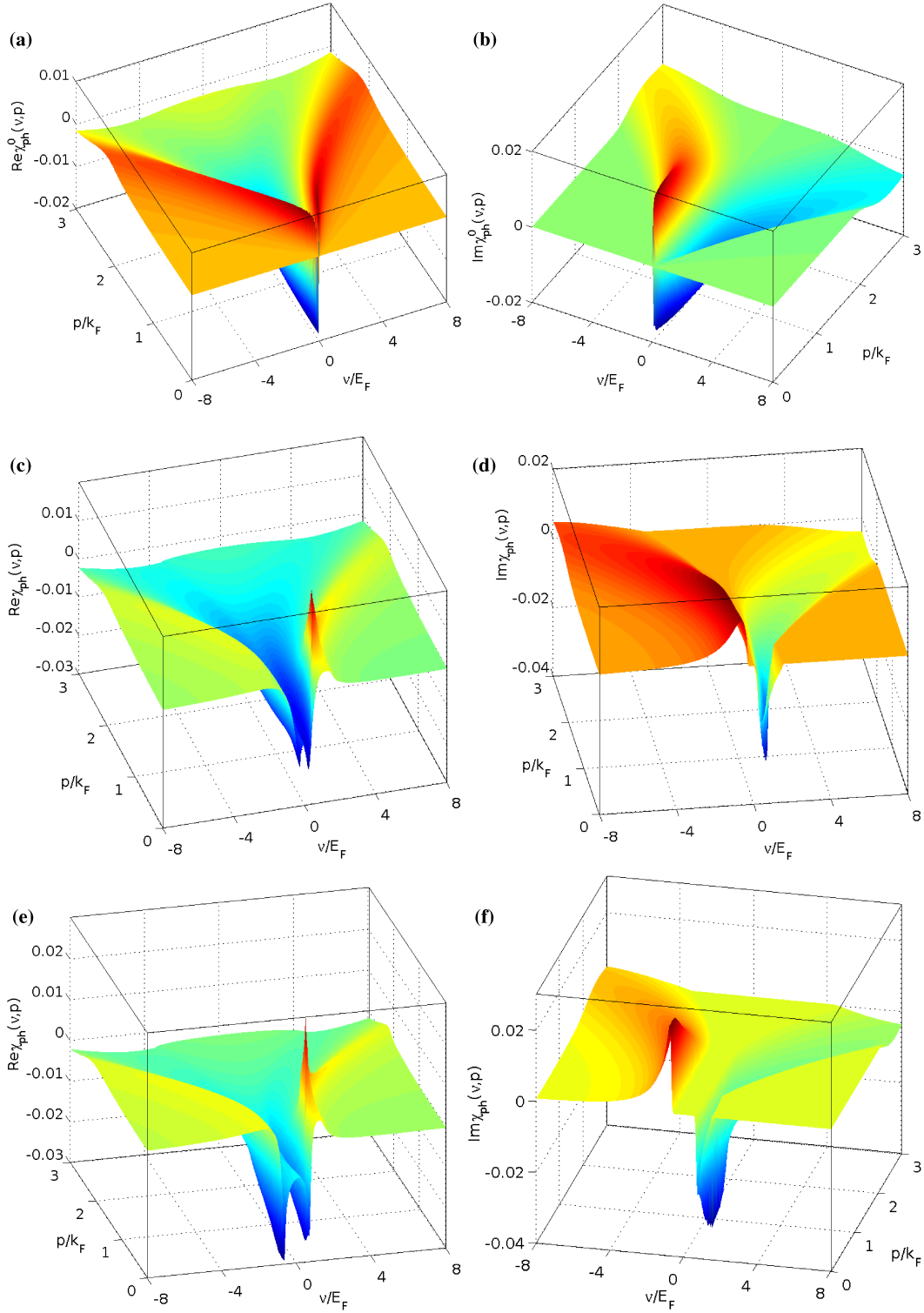


Figure 3. (Color online) 3D plots of the real (a,c,e) and imaginary (b,d,f) parts of the particle-hole pair susceptibility χ_{ph} with (c-f) and without (a,b) the self-energy feedback, calculated at T_c (a-d) and $0.1T_c$ (e,f) in the unitary limit. Here T_c is calculated using the pairing fluctuation theory without the particle-hole channel contributions. While the undressed $\chi_{\text{ph}}^{0R}(\nu, p)$ has a simple symmetry under $\nu \rightarrow -\nu$, the dynamic structure of $\chi_{\text{ph}}^R(\nu, p)$ is much more complex. In both cases, the real and imaginary parts have very strong dependencies on the total frequency ν and total momentum p . $\chi_{\text{ph}}^R(\nu, p)$ shows strong gap effects both at T_c and low T . In units of E_F , the parameters are: $T_c = 0.256$, $\mu(T_c) = 0.62$, $\Delta(T_c) = 0.64$, $\mu(0.1T_c) = 0.59$, and $\Delta(0.1T_c) = 0.69$.

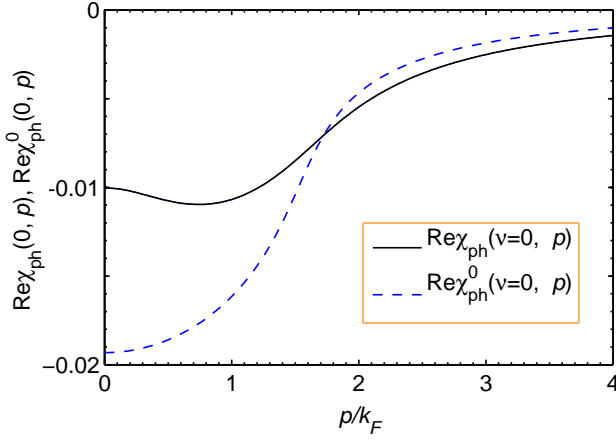


Figure 4. (Color online) Strong momentum dependence of the real part of the particle-hole susceptibility at zero frequency $\nu = 0$ in the unitarity limit, with (black curve) and without (blue dashed curve) self-energy feedback, calculated at $T = 0.3T_c$, where $T_c = 0.256E_F$. While the undressed $\chi_{ph}^{0r}(0, p) = \text{Re } \chi_{ph}^0(0, p)$ shows a simple monotonic behavior, the dressed susceptibility $\chi_{ph}(0, p) = \text{Re } \chi_{ph}(0, p)$ has a nonmonotonic p dependence, and a substantially reduced value at $p = 0$. This reduction derives from the gap effect in the Green's function $G(K)$. Namely, $\chi_{ph}'(0, p)$ seriously overestimated particle-hole fluctuations.

fully dressed Green's function. In other words, by neglecting the feedback effect, the bare $\chi_{ph}^0(P)$ misses this important dynamic structure. The plots of χ_{ph}^{0R} at $0.1T_c$ (not shown) is very similar to its $T = T_c$ counterpart shown in Figs. 3(a) and 3(b), except that the peaks become sharper. Comparing Figs. 3(e) and 3(f) with 3(c) and 3(d), the gap induced structures become much more pronounced. For example, for $p = 0$, the range of ν in which $\chi_{ph}''(\nu, 0) = 0$ becomes much wider at low T .

More quantitatively readable two-dimensional plots are presented in the Appendix. There we study in detail the effect of temperature and interaction strength on the particle-hole susceptibility, and how it behaves as a function of frequency ν for fixed momentum p or as a function of total momentum p for fixed frequency ν .

In Fig. 4, we plot systematically the zero frequency value of the real part of the particle-hole pair susceptibility as a function of total momentum p , with and without the feedback effect. The curves are computed at a relatively low $T = 0.3T_c$ at unitarity. Due to the large excitation gap $\Delta = 0.69E_F$, at $p = 0$, the value $\chi_{ph}'(0, 0)$ with the feedback is strongly suppressed from its undressed counterpart, $\chi_{ph}^{0r}(0, 0)$. In other words, *the neglect of the self-energy feedback in $\chi_{ph}^{0r}(0, 0)$ leads to serious over-estimate of the particle-hole channel contributions*. At the same time, $\chi_{ph}'(0, p)$ exhibits a more complex, nonmonotonic dependence on p than $\chi_{ph}^{0r}(0, p)$. In both cases, the momentum dependence is strong.

From Figs. 3 and 4, as well as the Appendix, one can readily see that the particle-hole susceptibility $\chi_{ph}^R(\nu, p)$ has very strong dependencies on both frequency and momentum, as well as the temperature and interaction strength.

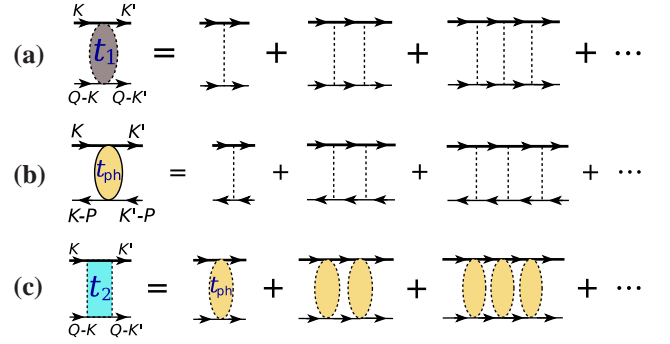


Figure 5. (Color online) Feynman diagrams showing the particle-hole effect on fermion pairing, in the presence of self-energy feedback. (a) Particle-particle T matrix $t_1(Q)$, with external four momenta labeled. (b) Particle-hole T matrix $t_{ph}(P)$, with $P = K + K' - Q$ being the total particle-hole 4-momentum. (c) An effective, composite particle-particle T -matrix, $t_2(Q)$, with the contribution from the particle-hole channel included. Here different shadings represent different T matrices.

C. Induced interaction – beyond the lowest order

Figure 3(b), in the absence of the self-energy feedback effect, is in fact the lowest order induced interaction, considered in GMB and most others in the literature:

$$U_{\text{ind}}^0(P) = -U^2 \chi_{ph}^0(P). \quad (20)$$

Diagrams of the same order but between fermions of the same spin vanish.

Let us first re-plot the particle-particle scattering T -matrix in Fig. 5(a); this is just t_{pg} in Fig. 1 but with external legs, which we here refer to as $t_1(Q)$. We have

$$t_1(Q) = \frac{1}{U^{-1} + \chi(Q)}. \quad (21)$$

Now we consider the contribution of an infinite particle-hole ladder series, as shown in Fig. 5(b). Such contribution should be added to the bare interaction U . The summation of the series of particle-hole ladder diagrams gives rise to the T -matrix in the particle hole channel,

$$t_{ph}(P) = \frac{U}{1 + U \chi_{ph}(P)} = \frac{1}{U^{-1} + \chi_{ph}(P)}. \quad (22)$$

At $Q = 0$, this gives the overall effective pairing interaction,

$$U_{\text{eff}}(K, K') = t_{ph}(K + K') = U + U_{\text{ind}} = \frac{U}{1 + U \chi_{ph}(K + K')}, \quad (23)$$

where K and K' are the incoming and outgoing 4-momenta of the scattering particles in the COM reference frame. The induced interaction is thus given by

$$U_{\text{ind}}(P) = t_{ph}(P) - U = -\frac{U^2 \chi_{ph}(P)}{1 + U \chi_{ph}(P)}, \quad (24)$$

with $P = K + K'$. Upon Taylor expanding the denominator by treating $U\chi_{\text{ph}}$ as a small parameter, one readily notice that the leading term is just the numerator. This would be the counterpart lowest induced interaction in our theory, except that we always consider the self energy feedback effect.

It is evident that the T matrices in the particle-particle channel and the particle-hole channel share the same lowest order term, U . Both T matrices can be regarded as a renormalized interaction, but in different channels. What we need is to replace the bare U in one of the two T matrices with the other T matrix. The results are identical, which we call t_2 . Shown in Fig. 5(c) is the regular particle-particle channel T matrix $t_1(Q)$ with U replaced by the particle-hole channel T matrix $t_{\text{ph}}(P)$ (with twisted external legs), where $P = K + K' - Q$. In other words, we replace U^{-1} with $t_{\text{ph}}^{-1}(P) = U^{-1} + \chi_{\text{ph}}(P)$ in Eq. (21), and formally obtain

$$t_2(Q) = \frac{1}{U^{-1} + \chi_{\text{ph}}(K + K' - Q) + \chi(Q)}. \quad (25)$$

Unfortunately, since $U_{\text{eff}}(K, K')$ is *not* a separable potential, one *cannot* obtain a simple summation in the form of Eq. (25). This can also be seen from the extra dependence on K and K' on the right hand side of the equation. Certain averaging process has to be done to arrive at such a simple summation, as will be shown below.

D. Gap equation from self-consistency condition in mean-field treatment

The dependence of $U_{\text{eff}}(P)$ on external momenta via $P = K + K' - Q$ presents a complication in the gap equation. This can be seen through the self consistency condition in the mean field treatment, even though we do not use mean field treatment in our calculations. Writing the interaction $V_{K,K'} = U_{\text{eff}}(K + K')$ for $Q = 0$, i.e., zero total pair 4-momentum, we have

$$\begin{aligned} \Delta_K &= \sum_{K'} V_{K,K'} \langle c_{K'} c_{-K'} \rangle \\ &= - \sum_{K'} \frac{U}{1 + U\chi_{\text{ph}}(K + K')} \frac{\Delta_{K'}}{(i\omega_{l'})^2 - E_{K'}^2}, \end{aligned} \quad (26)$$

where we have used the mean-field result $\langle c_{K'} c_{-K'} \rangle = G(K')G_0(-K')\Delta_{K'}$. Equivalently, this can be written as

$$\Delta_{\mathbf{k}, i\omega_l} = - \sum_{K'} \frac{U}{1 + U\chi_{\text{ph}}(i\omega_l + i\omega_{l'}, \mathbf{k} + \mathbf{k}')} \frac{\Delta_{\mathbf{k}', i\omega'}}{(i\omega')^2 - E_{K'}^2}. \quad (27)$$

Note that, due to the dynamic character of $\chi_{\text{ph}}(K + K')$, both the gap Δ_K and the quasiparticle dispersion E_K acquire a dynamical frequency dependence. The gap also develops a momentum dependence, which is originally absent for a contact potential.

We can express $U_{\text{eff}}(P)$ in terms of its retarded analytical continuation, as follows:

$$U_{\text{eff}}(P) = U + \int_{-\infty}^{\infty} \frac{d\nu}{2\pi} \frac{-2 \text{Im} U_{\text{eff}}^R(\nu, \mathbf{p})}{i\nu_n - \nu}, \quad (28)$$

where the second term is just the induced interaction,

$$\text{Im} U_{\text{eff}}^R(\nu, \mathbf{p}) = \frac{\chi_{\text{ph}}''(\nu, \mathbf{p})}{(U^{-1} + \chi_{\text{ph}}')^2 + (\chi_{\text{ph}}'')^2}. \quad (29)$$

Then we have

$$\Delta_{\mathbf{k}, i\omega_l} = U \sum_{K'} \frac{\Delta_{\mathbf{k}', i\omega_{l'}}}{(i\omega_{l'})^2 - E_{K'}^2} - \int_{-\infty}^{\infty} \frac{d\nu}{\pi} \frac{\text{Im} U_{\text{eff}}^R(\nu, \mathbf{k} + \mathbf{k}')}{i\omega_l + i\omega_{l'} - \nu}. \quad (30)$$

The particle-hole channel effect is contained in the 2nd term, without which this would be just the gap equation without the particle-hole channel, and admit a constant gap solution. Without further approximation, the complex dynamic structure of $\chi_{\text{ph}}(P)$ will inevitably render it very difficult to solve the gap equation.

E. Pairing instability condition in the presence of particle-hole channel effect

In order to obtain a simple form as Eq. (25), we have to average out the dependence of $U_{\text{eff}}(K, K')$ on K and K' . Indeed, an average of $\chi_{\text{ph}}(\nu, p)$ has been performed in the literature on (and only on) the Fermi surface [61]. For the frequency part, here we follow the literature and take $i\nu_n = i\omega_l + i\omega_{l'} = 0$. From Fig. 3, one can see that this is where the imaginary part $\chi_{\text{ph}}''(\nu, p) = 0$ for all p and thus the effective interaction $U_{\text{eff}}(K, K')$ is purely real. For the momentum part, we choose on-shell, elastic scattering, i.e., $k = k'$, and then average over scattering angles:

$$p = |\mathbf{k} + \mathbf{k}'| = k\sqrt{2(1 + \cos\theta)}, \quad (31)$$

where θ is the angle between \mathbf{k} and \mathbf{k}' . It is the off-shell scattering processes which lead to imaginary part and nontrivial frequency dependence in $\chi_{\text{ph}}^R(\nu, p)$ and the order parameter. Further setting $k = k_\mu$ and averaging only on the Fermi surface is the averaging process used in all papers we can find about induced interactions in the literature. We refer to this as *level 1* averaging. In this paper, we also perform a *level 2* average, over a range of k such that the quasiparticle energy $E_{\mathbf{k}} \in [\min(E_{\mathbf{k}}), \min(E_{\mathbf{k}}) + \Delta]$. Here $\min(E_{\mathbf{k}}) = \Delta$ if $\mu > 0$, or $\min(E_{\mathbf{k}}) = \sqrt{\mu^2 + \Delta^2}$ if $\mu < 0$. The basic idea is that according to the density of states of a typical s -wave superconductor, the states within the energy range $E_{\mathbf{k}} \in [\Delta, 2\Delta]$ are most strongly modified by pairing. It should be pointed out that in the BEC regime, this range can become very large.

Upon averaging of either level 1 or level 2, we drop out the complicated dynamical structure of $\chi_{\text{ph}}(\nu, p)$ and replace it by a constant $\langle \chi_{\text{ph}} \rangle$. For the purpose of comparison, we shall also perform the averaging on the undressed particle-hole susceptibility $\chi_{\text{ph}}^0(\nu, p)$ but will mostly show the result at level 1.

Shown in Fig. 6 are the angular averages of the particle-hole susceptibility at $\nu = 0$ as a function of momentum k under the above on-shell condition, $k = k'$. Here we only

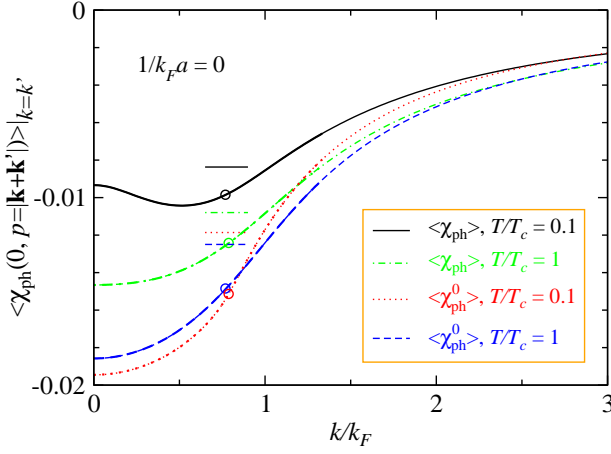


Figure 6. (Color online) Angular average of the on-shell particle-hole susceptibility, $\langle \chi_{ph}(0, p = |\mathbf{k} + \mathbf{k}'|) \rangle|_{k=k'}$ at $\nu = 0$ as a function of momentum k/k_F , under the condition $k = k'$, calculated at unitarity for different temperatures $T = 0.1T_c$ (black solid curve) and $T = T_c$ (green dot-dashed curve), in units of k_F^3/E_F . Also plotted is its undressed counterpart, $\langle \chi_{ph}^0(0, p = |\mathbf{k} + \mathbf{k}'|) \rangle$, which shows a serious over-estimate due to the neglect of the self-energy feedback. Here $T_c = 0.256E_F$ and associated gap and μ values are calculated without the particle-hole channel effect. The open circles on each curve denote level 1 average, i.e., $k = k_\mu$. The vertical axis readings of the horizontal short bars indicate the corresponding values of level 2 average. The thick section of each curve indicates the range of k used for level 2 averaging. Clearly, there are strong temperature and k dependencies in both $\langle \chi_{ph}(0, p) \rangle$ and $\langle \chi_{ph}^0(0, p) \rangle$. The (absolute) values of Level 2 average are substantially smaller than their level 1 counterpart.

show the unitary case at two different temperatures, $T = T_c$ and low $T = 0.1T_c \ll T_c$. For the purpose of comparison, we plot the result for both the dressed and undressed particle-hole susceptibility. The curves show strong momentum dependencies. For $\langle \chi_{ph}^0(0, p) \rangle$, it is monotonically increasing, whereas for $\langle \chi_{ph}(0, p) \rangle$, it exhibits nonmonotonic k dependence at low T . Both dressed and undressed particle-hole susceptibilities have a temperature dependence, and this dependence is much stronger for the former. This can be attributed mainly to the temperature dependence of $\Delta(T)$ in $\langle \chi_{ph}(0, p) \rangle$, while $\langle \chi_{ph}^0(0, p) \rangle$ depends on T only via $\mu(T)$.

The open circles on each curve represent the level 1 average, i.e., the values at $k = k_\mu$. At the same time, the vertical axis readings of the short horizontal bars correspond to the level 2 average, while the thick segments of each curve represents the range of k used for level 2 averaging. Figure 6 shows that the (absolute) values of the level 2 average are significantly smaller than their level 1 counterpart. The level 1 average $\langle \chi_{ph}(0, p) \rangle$ is essentially temperature independent (see the red and blue circles). In addition, it is evident that *the neglect of self-energy feedback has caused $\langle \chi_{ph}^0(0, p) \rangle$ to seriously over-estimate the contribution of particle-hole channel.*

Similar plot for $1/k_F a = 0.5$ (Fig. 15 in the Appendix) exhibits a much stronger T dependence. In that case, μ is very close to 0 albeit still positive. As a consequence, the particle-hole susceptibility is much smaller than that shown in

Fig. 6.

Now with this frequency and momentum independent $\chi_{ph}(\nu, p) \approx \langle \chi_{ph} \rangle$, we can easily carry out the simple geometric summation for t_2 :

$$t_2(Q) = \frac{1}{U^{-1} + \langle \chi_{ph} \rangle + \chi(Q)}. \quad (32)$$

Therefore, the Thouless criterion for pairing instability leads to the gap equation:

$$U^{-1} + \langle \chi_{ph} \rangle + \chi(0) = 0, \quad (33)$$

namely,

$$-\left(\frac{m}{4\pi a} + \langle \chi_{ph} \rangle\right) = \sum_{\mathbf{k}} \left[\frac{1 - 2f(E_{\mathbf{k}})}{2E_{\mathbf{k}}} - \frac{1}{2\epsilon_{\mathbf{k}}} \right]. \quad (34)$$

As will be shown later, $\langle \chi_{ph} \rangle$ is always negative. Therefore, the particle-hole channel effectively reduces the strength of the pairing interaction.

In the weak coupling limit ($1/k_F a = -\infty$), $\Delta \rightarrow 0$, $T \lesssim T_c \ll T_F$, then $\langle \chi_{ph} \rangle$ and $\langle \chi_{ph}^0 \rangle$ become equal, for either level of averaging. We have

$$\begin{aligned} \langle \chi_{ph} \rangle &= \int_{-1}^1 dx \int_0^\infty \frac{k dk}{4\pi^2} \frac{m}{p} f(\xi_{\mathbf{k}}) \ln \left| \frac{2k - p}{2k + p} \right|_{p=k_F \sqrt{2(1+x)}} \\ &\approx N(0) \int_{-1}^1 dx \int_0^1 \frac{\tilde{k} d\tilde{k}}{2\tilde{p}} \ln \left| \frac{2\tilde{k} - \tilde{p}}{2\tilde{k} + \tilde{p}} \right| \\ &= -\frac{1 + 2 \ln 2}{3} N(0) = 0.02015 \frac{k_F^3}{E_F}, \end{aligned} \quad (35)$$

where $\tilde{k} = k/k_F$, $\tilde{p} = p/k_F = \sqrt{2(1+x)}$, $x = \cos \theta$, and $N(0) = mk_F/2\pi^2 \hbar^2$ is the density of state at the Fermi level. Here we have approximated the Fermi function with its $T = 0$ counterpart, with a step function jump at the Fermi level.

In the weak interaction limit, the BCS result for T_c is $T_c^{BCS}/E_F = (8/\pi) e^{\gamma-2} e^{1/N(0)U}$, where $\gamma \approx 0.5772157$ is the Euler's constant. Equation (33) implies a replacement of $1/U$ by $1/U + \langle \chi_{ph} \rangle$. In this way, the new transition temperature T_c is given by

$$\frac{T_c}{T_c^{BCS}} = e^{\langle \chi_{ph} \rangle / N(0)} = (4e)^{-1/3} \approx 0.45, \quad (36)$$

and the same relation holds for zero T gap,

$$\frac{\Delta}{\Delta^{BCS}} = (4e)^{-1/3}. \quad (37)$$

This result is in *quantitative* agreement (to the leading order) with that of GMB [61] and others [63] in the literature. Note that in our work, as well as in that of Yin and coworkers [66], the average particle-hole susceptibility $\langle \chi_{ph} \rangle$ is added to $1/U$ or $m/4\pi a$. In other works [63–65], only the lowest order particle-hole diagram is considered so that their induced interaction $U_{ind}^0 = -U^2 \langle \chi_{ph}^0 \rangle$ is added to U . Therefore, these works have to rely on the assumption $N(0)U \ll 1$ and the validity of the BCS mean-field result in order to obtain the result

of Eq. (36). Away from the weak interaction regime, a full summation of the particle-hole T matrix becomes necessary.

While the results from all different treatment seem to agree quantitatively in the weak coupling limit, we expect to see significant departures as the pairing interaction strength increases, especially in the unitary regime.

With the overall effective interaction U_{eff} , the self energy, as obtained from $\Sigma(K) = \sum_Q t_2(Q)G_0(Q-K)$, will follow the same form as Eq. (8) although the gap values will be different. Therefore, the fermion number equation will also take the same form as Eq. (10). Furthermore, the pseudogap equation, given by $\Delta_{\text{pg}}^2 = -\sum_Q t_2(Q)$, will also take the same form as Eq. (7).

Equations (10), (7), and (34) now form a new closed set, and will be solved to investigate the effect of the particle-hole channel.

Note that in a *very dilute* Fermi gas shifting $m/4\pi a$ by $\langle\chi_{\text{ph}}\rangle$ has no significant influence in experimental measurement of the s -wave scattering length a , because $\langle\chi_{\text{ph}}\rangle$ has dimension $[k_F]^3/[E_F] = [k_F]$ and thus vanishes as $k_F \rightarrow 0$ in the zero density limit. However, a finite k_F will indeed shift the resonance location except at very high T where $\mu < 0$. In Ref. [56], from which the scattering lengths are often quoted for ^6Li , the actual density is comparable or even higher than that in most typical Fermi gas experiments. Therefore, the particle-hole channel may play an important role.

Here we propose that this particle-hole channel effect may be verified experimentally by precision measurement of the magnetic field B at the exact Feshbach resonance point as a function of density or k_F at low T . The zero density field B_0 can be obtained by extrapolation. Then one should have the field detuning $\delta B = B - B_0 \propto k_F$. Because different theories predict a very different value of $\langle\chi_{\text{ph}}\rangle$ at unitarity, the measured field detuning can thus be used to quantify $\langle\chi_{\text{ph}}\rangle$ and test these theories. In principle, one may experimentally measure $\langle\chi_{\text{ph}}\rangle$ through the entire BCS-BEC crossover. For a Fermi gas in a trap, the trap inhomogeneity leads to a distribution of k_F . Instead of a uniform shift, this inhomogeneity will spread out the unitary point at zero density into a narrow band at finite density. The band width and mean shift are both expected to be proportional to k_F . Such effect deserves further investigation.

III. NUMERICAL RESULTS AND DISCUSSIONS

A. Effect of particle-hole channel on BCS-BEC crossover

In this section, we will investigate the effect of the particle-hole channel on the BCS-BEC crossover behavior, in terms of zero temperature gap $\Delta(0)$, T_c and their ratio.

First, in Fig. 7, we show the effect on the zero T gap by comparing the calculated result with and without the particle-hole channel contributions. Shown respectively in panel (a) and (b) are plots of the zero T gap Δ and the corresponding particle-hole susceptibility (with a minus sign) as a function of $1/k_F a$. The black solid line in Fig. 7(a) is the result without the particle-hole channel effect, whereas the other curves

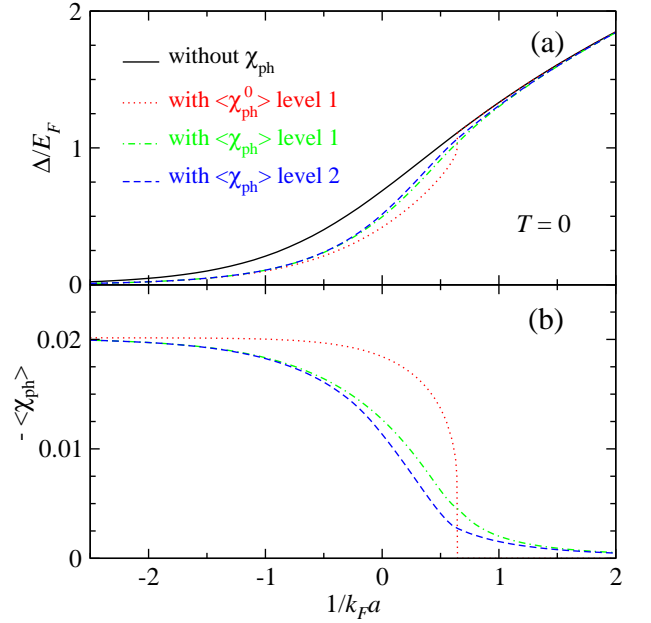


Figure 7. (Color online) Effect of the particle-hole channel contributions on the zero temperature gap in BCS-BEC crossover. In (a), the black solid curve is the gap without the particle-hole effect. The rest curves are calculated with the particle-hole channel effect but at different levels, i.e., using undressed particle-hole susceptibility $\langle\chi_{\text{ph}}^0\rangle$ with level 1 averaging (red dotted line), dressed particle-hole susceptibility $\langle\chi_{\text{ph}}\rangle$ with level 1 (green dot-dashed curve) and level 2 (blue dashed line) averaging, respectively. The corresponding values of the average particle-hole susceptibility with a minus sign are plotted in (b), in units of k_F^3/E_F . The particle-hole channel effect can be essentially neglected beyond $1/k_F a > 1.5$.

are calculated with the effect at different levels of approximation. The (red) dotted curve are calculated using the undressed susceptibility $\langle\chi_{\text{ph}}^0\rangle$ at average level 1. The (green) dot-dashed and (blue) dashed curves are calculated using the dressed particle-hole susceptibility $\langle\chi_{\text{ph}}\rangle$ with level 1 (green dot-dashed curve) and level 2 (blue dashed line) averaging, respectively. The level 2 result shows a slightly weaker particle-hole channel effect, as can be expected from Fig. 6.

One feature that is easy to spot is that the undressed particle-hole susceptibility $\langle\chi_{\text{ph}}^0\rangle$ has a very abrupt shut-off where the chemical potential μ changes sign. As a result, the corresponding (red dotted) curve of the gap also merges abruptly with the (black solid) gap curve calculated without particle-hole channel effect. This is *not unexpected* as one can see from Eq. (18) that $\langle\chi_{\text{ph}}^0\rangle = 0$ at $T = 0$ for $\mu \leq 0$. Furthermore, Eq. (17) implies that $\langle\chi_{\text{ph}}^0\rangle$ approaches zero at $\mu = 0$ abruptly with a finite slope as k_μ does. In contrast, with the self-energy feedback included, either level 1 (green dot-dashed curves) or level 2 (blue dashed curves) average of $\langle\chi_{\text{ph}}\rangle$ approaches 0 smoothly as the BEC regime is reached. Consequently, in Fig. 7(a), the (green) dot-dashed and (blue) dashed curves approach the (black) solid curve very gradually. It is also worth pointing out that the difference between level 1 and level 2 average of $\langle\chi_{\text{ph}}\rangle$ is less dramatic than that between

$\langle\chi_{\text{ph}}\rangle$ and the undressed $\langle\chi_{\text{ph}}^0\rangle$. Indeed, the (green) dot-dashed and (blue) dashed curves are very close to each other.

The abrupt shut-off of $\langle\chi_{\text{ph}}^0\rangle$ at $\mu = 0$ is determined by the step function characteristic of the Fermi function at $T = 0$. At finite T , this shut-off will become smoother with an exponential tail on the BEC side.

In the unitary regime, especially for $1/k_{\text{F}}a \in [-0.5, +0.5]$, the particle-hole susceptibility is strongly over-estimated by the undressed $\langle\chi_{\text{ph}}^0\rangle$ in comparison with the dressed $\langle\chi_{\text{ph}}\rangle$. In this regime, both the gap and the underlying Fermi surface (as defined by the chemical potential) are large, so that neglecting the self-energy feedback leads to a strong over-estimate of $\langle\chi_{\text{ph}}^0\rangle$, because the large gap serves to suppress particle-hole fluctuations.

From Fig. 7, we conclude that the particle-hole effect diminishes quickly as the Fermi gas is tuned into the BEC regime with increasing pairing interaction strength. Beyond $1/k_{\text{F}}a > 1.5$, the effect can essentially be neglected. For the level 1 average of the undressed particle-hole susceptibility, $\langle\chi_{\text{ph}}^0\rangle$, as has been done in the literature, this effect disappears immediately once the BEC regime (defined by $\mu < 0$) is reached, as far as the zero T gap is concerned.

As a consistency check, we notice that in the BCS limit, the average particle-hole susceptibility in all cases in Fig. 7(b) approaches the same asymptote, which is given by Eq. (35). This confirms our previous analytical analysis.

Next, we show in Fig. 8 the effect of the particle-hole channel on the behavior of T_c as well as the pseudogap at T_c . Figure 8(c) can be compared with Fig. 7(b). The curves for levels 1 and 2 average of $\langle\chi_{\text{ph}}\rangle$ in Fig. 8(c) are very similar to those in Fig. 7(b), with the values at $1/k_{\text{F}}a = 0$ slightly smaller. On the other hand, the curve for $\langle\chi_{\text{ph}}^0\rangle$ has a smooth thermal exponential tail in the BEC regime in Fig. 8(c). Thus, the pseudogap $\Delta(T_c)$ calculated using $\langle\chi_{\text{ph}}^0\rangle$ now merges back to the (black) solid curve smoothly.

Similar to the zero T gap case in Fig. 7, the difference in the effect on T_c and $\Delta(T_c)$ between level 1 and level 2 averaging mainly resides in the unitary regime, and is less dramatic than that between undressed and dressed particle-hole susceptibility. Again, *the undressed particle-hole susceptibility gives rise to an overestimate of the particle-hole channel effect*.

In all cases, the particle-hole susceptibility becomes negligible in the BEC regime. The effect of the particle-hole channel shifts the T_c and $\Delta(T_c)$ curve towards larger $1/k_{\text{F}}a$, although the amount of shift clearly depends on the value of $1/k_{\text{F}}a$.

Now we study the effect of the particle-hole channel on the ratio $2\Delta(0)/T_c$. It suffices to consider the mean-field ratio, $2\Delta(0)/T_c^{\text{MF}}$, since $2\Delta(0)/T_c$ obviously will deviate from the weak coupling BCS result when pairing fluctuations are included in the crossover and BEC regimes. From Fig. 6, we see a strong T dependence of the particle-hole susceptibility. Therefore, the effect on T_c^{MF} and on zero T gap $\Delta(0)$ are different, as can be seen roughly from Figs. 7 and 8.

In Fig. 9, we plot this mean-field ratio as a function of $1/k_{\text{F}}a$ with (black solid curve) and without (blue dashed curve) the particle-hole channel effect. Here the particle-hole susceptibility $\langle\chi_{\text{ph}}\rangle$ is calculated with level 2 averaging. In the

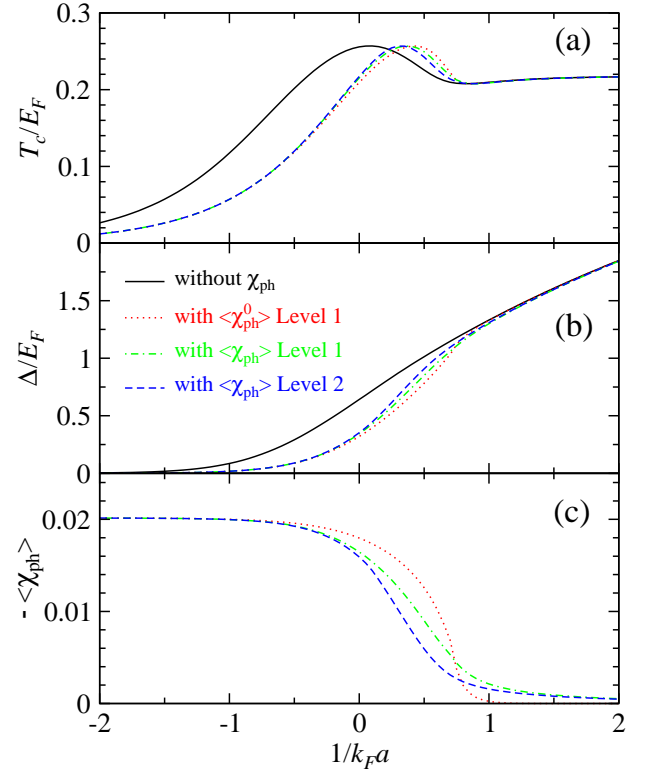


Figure 8. (Color online) Effect of the particle-hole channel contributions on T_c and the pseudogap Δ at T_c in BCS-BEC crossover. In (a) and (b), the black solid curves are calculated without the particle-hole effect. The rest curves are calculated with the particle-hole channel effect but at different levels, using undressed particle-hole susceptibility $\langle\chi_{\text{ph}}^0\rangle$ with level 1 averaging (red dotted line), dressed particle-hole susceptibility $\langle\chi_{\text{ph}}\rangle$ with level 1 (green dot-dashed curve) and level 2 (blue dashed line) averaging, respectively. The corresponding values of the average particle-hole susceptibility with a minus sign are plotted in (c), in units of $k_{\text{F}}^3/E_{\text{F}}$. The particle-hole channel effect can be essentially neglected beyond $1/k_{\text{F}}a > 1.5$.

$1/k_{\text{F}}a \rightarrow -\infty$ limit, the ratio is unaffected by the particle-hole channel. As $1/k_{\text{F}}a$ increases, the contribution of the particle-hole channel causes this ratio to increase gradually. At $1/k_{\text{F}}a = -4$, which is still a very weak pairing case, the ratio is already slightly larger. The effect is most dramatic in the unitary regime, since further into the BEC regime, $\langle\chi_{\text{ph}}\rangle$ will vanish gradually. It is worth noting that even without the particle-hole channel, the ratio $2\Delta(0)/T_c^{\text{MF}}$ starts to decrease from its weak coupling limit, $2\pi e^{-\gamma} \approx 3.53$.

Finally, we estimate the shift in Feshbach resonance positions. From Figs. 7 and 8, we find that χ_{ph} does not necessarily diminish as T increases except at very high T (where μ becomes negative, so that $|\chi_{\text{ph}}|$ will decrease exponentially with T .) In fact, this can be understood because $\Delta(T)$ decreases with T so that $|\chi_{\text{ph}}|$ increases. We take $\langle\chi_{\text{ph}}\rangle = -0.01k_{\text{F}}^3/E_{\text{F}} = -0.01(2mk_{\text{F}}/\hbar^2)$. According to Eq. (34), the shift in $1/a$ is $\delta(1/a) = -4\pi\hbar^2\langle\chi_{\text{ph}}\rangle/2m = 0.08\pi k_{\text{F}}$. In other words, the dimensionless shift $\delta(1/k_{\text{F}}a) = 0.25$, which is independent of density and is no longer negligible. This is in good agreement with the actual shift 0.32 of

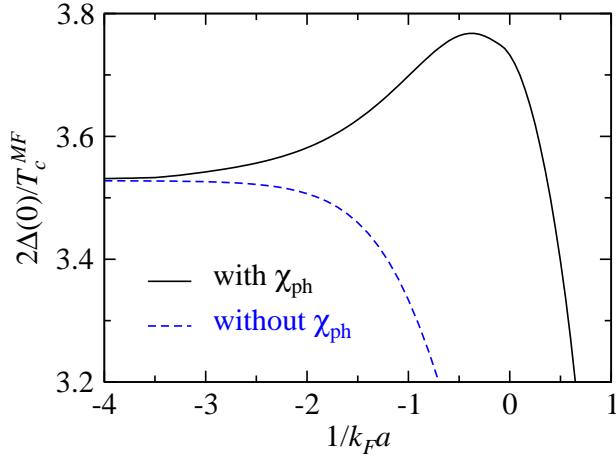


Figure 9. (Color online) Effect of the particle-hole channel contributions on the ratio $2\Delta(0)/T_c^{MF}$ in BCS-BEC crossover. Shown is the mean-field ratio calculated with (black solid curve) and without (blue dashed curve) the particle-hole channel contributions. Here the particle-hole susceptibility $\langle\chi_{ph}\rangle$ is calculated with level 2 averaging.

the peak location of the T_c curve in Fig. 8(a). For a typical $T_F = 1\mu\text{K}$ in ^6Li , using the approximate expression $a = a_{bg}[1 - W/(B - B_0)]$, we obtain the shift in resonance position $\delta B_0 = -0.08W/(k_F a_{bg}) = 7.8\text{G}$. Here for the lowest two hyperfine states, the resonance position $B_0 = 834.15\text{G}$, the resonance width $W = 300\text{G}$, and the background scattering length $a_{bg} = -1405a_0$, with $a_0 = 0.528\text{\AA}$. Clearly, the shift δB_0 is not small. In reality, one needs to solve self-consistently the equation $m/(4\pi a) + \langle\chi_{ph}\rangle = 0$, and take care of the trap inhomogeneity. These will likely make the actual average shift smaller.

The susceptibility χ_{ph} calculated with and without the self energy feedback differs by roughly a factor of 2 at unitarity. This can be used to test different theories, as mentioned earlier.

A question arises naturally as to whether the particle-hole channel effect has already been included in the experimentally measured scattering length a , since, after all, the measurements of a such as those in Ref. [56] were carried out at densities comparable to typical Fermi gas experiments. This also depends on whether the temperature was high enough during the measurements.

B. Critical temperature T_c at unitarity

Finally, we compare our result on the critical superfluid transition temperature T_c/E_F for a 3D homogeneous Fermi gas at unitarity with those reported in the literature. From Fig. 8, we read $T_c/E_F = 0.217$ using level 2 average of $\langle\chi_{ph}\rangle$. And the maximum $T_c \approx 0.257$ now occurs at $1/k_F a \approx 0.32$, on the BEC side. The level 1 average of $\langle\chi_{ph}^0\rangle$ yields a slightly lower value, $T_c/E_F = 0.209$. However, we emphasize that the level 2 average of $\langle\chi_{ph}\rangle$ is more reasonable. Note that as in the theory without particle-hole channel effect, we

have dropped out the incoherent part of the self-energy from particle-particle scattering. Inclusion of the incoherent part is necessary in order to obtain the correct value of the β factor.

Hu and coauthors [81, 82] have been claiming to be able to obtain the correct value of the β factor, using an NSR-based approach, *without including the particle-hole channel*. Obviously, their claim will breakdown when the particle-hole channel is included.

The value of T_c for a homogeneous Fermi gas at unitarity has been under intensive study over the past few years. Without the particle-channel effect, using the pairing fluctuation theory, we previously reported a value of $T_c/E_F = 0.255$ for a short range Gaussian potential (using a two-channel model with a cutoff momentum $k_0/k_F = 80$) [29] or 0.256 for an exact contact potential. In all cases, the maximum T_c occurs very close to but slightly on the BEC side of the unitarity. The original NSR theory [3] predicted $T_c/E_F = 0.222$. Haussmann *et al.* [83] found 0.16, using a conserving approximation which involves only dressed Green's functions. However, this theory did not contain a pseudogap at T_c and exhibited unphysical non-monotonic first order like behavior in the temperature dependence of entropy $S(T)$. Floerchinger *et al.* [84] found a high value of 0.264 even after including the particle-hole channel fluctuations. By including the induced interaction in an NSR-based treatment without self-energy feedback, Yin and coworkers [66] reported a value of 0.178. However, as shown above, the neglect of the pseudogap self energy feedback in Ref. [66] has caused a serious over-estimate of the contributions of the induced interaction. In addition, their work suffers all defects of the NSR theory, i.e., lack of self-consistency and neglect of the pseudogap effect.

Using the renormalization group method, Stoof and coworkers [85] obtained $T_c/E_F = 0.13$, lower than most other calculations. Troyer and coworkers [86] reported 0.152 using quantum Monte Carlo (QMC) simulations for lattice fermions at finite densities and then extrapolated to zero density limit. Using (and improved upon) the method of Ref. [86], Goulko and Wingate [87] found a higher value, 0.171. An even higher value would have been obtained had they used a quadratic fit to (and extrapolation of) their intermediate density data. Also using QMC, Akkineni *et al.* [88] recently reported a value of 0.245.

Experimentally, only T_c in a trap has been measured. The Duke group [71], in collaboration with Chen *et al.*, found $T_c/E_F = 0.27$ in a trap through a thermodynamic measurement in a unitary ^6Li gas. Later, the Duke group [89, 90] obtained 0.29 and 0.21 by fitting entropy and specific heat data with different formulas. At unitarity, it has been known that T_c/E_F in the trap is only slightly higher than its homogeneous counterpart. Therefore, these experimental values probably imply that the homogeneous value of T_c/E_F is about $0.25 \sim 0.19$. Our result, $T_c/E_F = 0.217$, is in reasonable agreement with these experiments. Recently, Ku *et al.* [91] reported $T_c/E_F \approx 0.167$ for a homogeneous Fermi gas by identifying the lambda-like transition temperature. Interestingly, if we take an constant $\delta\Sigma = -0.3E_F$ (half of the energy of a single spin down atom in a spin up Fermi sea [92]) as the incoherent

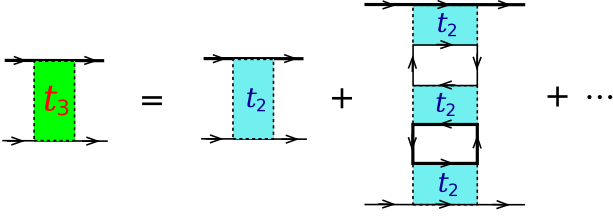


Figure 10. (Color online) Higher order T -matrix, t_3 , obtained by repeating the T -matrix t_2 .

part of the self energy in Eq. (6), T_c/E_F will be suppressed down to 0.174, close to this recent experimental value. Full numerical inclusion of $\delta\Sigma$ will be done in a future study.

C. Higher order corrections

In addition to non-ladder diagrams, which we have chosen not to consider, there seem to be a series of higher order corrections. For example, one can imagine repeating the T -matrix t_2 in the way shown in Fig. III B, and obtaining a higher order T -matrix t_3 . Such t_3 can then be repeated to obtain a higher order T -matrix t_4 , and so on. While one may argue these higher order T -matrices are indeed of higher order in bare interaction U , our experience with t_2 seems to imply that detailed study needs to be carried out before we jump to a conclusion on this. Indeed, even the lowest order so-called induced interaction U_{ind}^0 is one order higher in U than U itself.

IV. CONCLUSIONS

In summary, we have studied the effects of the particle-hole channel on BCS-BEC crossover and compared with lower level approximations. We include the self-energy feedback in the particle-hole susceptibility χ_{ph} , which leads to substantial differences than the result without self-energy feedback.

We have investigated the dynamic structure of χ_{ph} , and have discovered very strong temperature, momentum and frequency dependencies. Angular (as well as radial) average in the momentum space of the particle-hole susceptibility has been done in order to keep the equations manageable. We have performed the average at two different levels and also compared with the result calculated without including the self-energy feedback. We conclude that the level 2 averaging, i.e., both over angles and a range of momentum, is more reasonable. Computations of the particle-hole susceptibility without the self-energy feedback leads to an overestimate of the particle-hole channel effect.

In the weak coupling BCS limit, our result agrees, to the leading order, with that of GMB and others in the literature. Away from the weak coupling limit, $\Delta(0)$ and T_c are suppressed differently. We have also studied the ratio $2\Delta(0)/T_c^{\text{MF}}$ at the mean-field level and found that it is modified by the particle-hole fluctuations. The particle-hole channel effects diminish quickly once the system enters BEC

regime.

Without including the incoherent part of the self energy from particle-particle scattering, our present result on the critical temperature at unitarity yields $T_c/E_F \approx 0.217$, substantially lower than that obtained without the particle-hole effect. This value agrees reasonably well with some existing experimental measurement.

We have also made a falsifiable proposal that the particle-hole contribution can be measured by locating the Feshbach resonance positions as a function of k_F and that this can be used to test different theories.

To study more accurately the quantitative consequences of the dynamic structure of the particle-hole susceptibility, full-fledged numerical calculations are needed, without taking simple angular average and setting frequency $\nu = 0$. Further investigation is called for in order to determine whether higher order T -matrices will make a significant difference or not.

ACKNOWLEDGMENTS

This work is supported by NSF of China (grant No. 10974173), MOST of China (grant Nos. 2011CB921300 and 2011CC026897), the Fundamental Research Funds for the Central Universities of China (Program No. 2010QNA3026), Changjiang Scholars Program of the Ministry of Education of China, Qianjiang RenCai Program of Zhejiang Province (No. 2011R10052), and by Zhejiang University (grant No. 2009QNA3015).

Appendix A: Dynamic structure of the particle-hole susceptibility

In this Appendix, we will present a series of two-dimensional plots, in order to make the 3D data shown in Fig. 3 quantitatively easier to read.

First, we study the impact of temperature. We present in Fig. 11 the real and imaginary parts of $\chi_{\text{ph}}^R(\nu, 0)$ for different T from low to high in the unitary limit, $1/k_F a = 0$. To single out the temperature effect, here we take for all temperature $\Delta = 0.686$ and $\mu = 0.59$, which are their values calculated at $T = 0$ using the pairing fluctuation theory without the particle-hole channel effect. Evidently, beyond the point $\nu = \sqrt{\mu^2 + \Delta^2} + \mu = 1.49$, the imaginary part $\chi_{\text{ph}}''(\nu, 0)$ vanishes identically. Around $\nu = 0$, the lower bound of the range of ν where $\chi_{\text{ph}}''(\nu, 0)$ essentially vanishes changes from $\nu = -\Delta = -0.686$ at low T to $\nu = -(\sqrt{\mu^2 + \Delta^2} - \mu) = 0.315$ at high T . Meanwhile, its upper bound decreases continuously with T from $\nu = \Delta$ at low T to $\nu = 0$ at very high T . This numerical result agrees with our previous analysis. A comparison with the real part reveals that the peaks in $\chi_{\text{ph}}'(\nu, 0)$ correspond to the sharp rises in the plot of $\chi_{\text{ph}}''(\nu, 0)$ near these lower and upper bounds. This can also be seen from the Kramers-Kronig relation between the real and imaginary parts of $\chi_{\text{ph}}^R(\nu, 0)$.

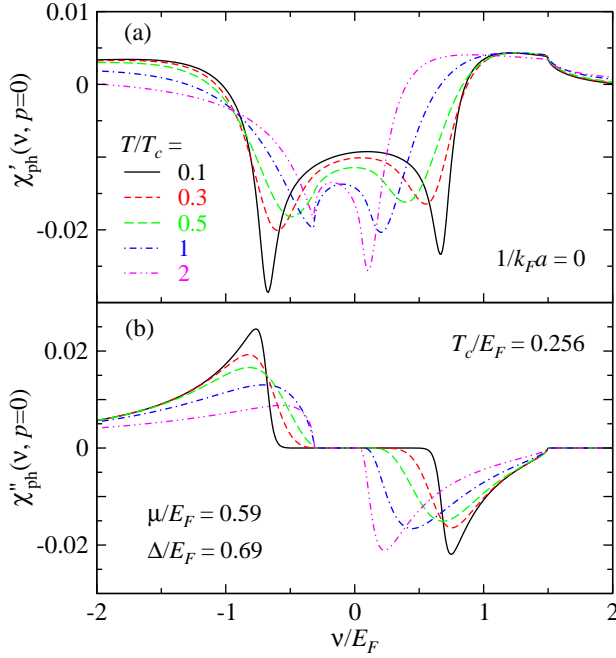


Figure 11. (Color online) The particle-hole susceptibility $\chi_{ph}^R(\nu, 0)$ at zero momentum p in the presence of self-energy feedback for different T (as labeled) at unitarity. To single out the temperature effect, we fix $\Delta = 0.686$ and $\mu = 0.59$ at their values at $T = 0$, calculated using the pairing fluctuation theory without the particle-hole channel effect.

In comparison, we have also studied the temperature evolution of the undressed $\chi_{ph}^{0R}(\nu, p)$. Shown in Fig. 12 is the result for $p = 0.1$. From Fig. 3, it is easy to see that one cannot plot the result for $p = 0$. This can also be seen from Eqs. (16) and (17). For finite p , say $p = 0.1$, the peaks at low T in both real and imaginary parts become more smeared out as T increases. Near $\nu = 0$, we see that $\chi_{ph}^{0R}(\nu, p = 0.1)$ is proportional to ν , in agreement with our previous analysis. $\chi_{ph}^{0R}(\nu, p)$ shows good symmetry about ν : $\chi_{ph}^{0R}(-\nu, p) = \chi_{ph}^{0R*}(\nu, p)$. There is no gap effects, of course.

Shown in Fig. 13 is the evolution of the particle-hole susceptibility $\chi_{ph}^R(\nu, 0)$ at total momentum $p = 0$ in the presence of feedback effect with increasing pairing strength. These curves are calculated at low temperature $T = 0.1T_c$. Here for each interaction strength, the parameters Δ , μ and T_c are calculated using the pairing fluctuation theory without the particle-hole channel effect. Around $\nu = 0$, the range within which the imaginary part vanishes is given by $|\nu| < \Delta$ for the $\mu > 0$ cases ($1/k_F a = -1$ through 0.5). For $1/k_F a = 1$, $\mu/E_F = -0.8$, the lower bound is given by $-(\sqrt{\mu^2 + \Delta^2} - \mu) = -2.35$ and its upper bound extends to ∞ since $\Delta = 1.33 > \sqrt{\mu^2 + \Delta^2} + \mu = 0.75$. It is obvious that this range becomes wider and wider with increasing pairing strength from BCS to BEC.

From Figs. 3(a) and 3(b), one readily notice that for the undressed $\chi_{ph}^{0R}(\nu, p)$, it is not appropriate to plot $\chi_{ph}^{0R}(\nu, p = 0)$ as a function of ν . Instead, one has to plot at a finite p , say, $p = 0.1k_F$, in order to study its temperature evolution. Our

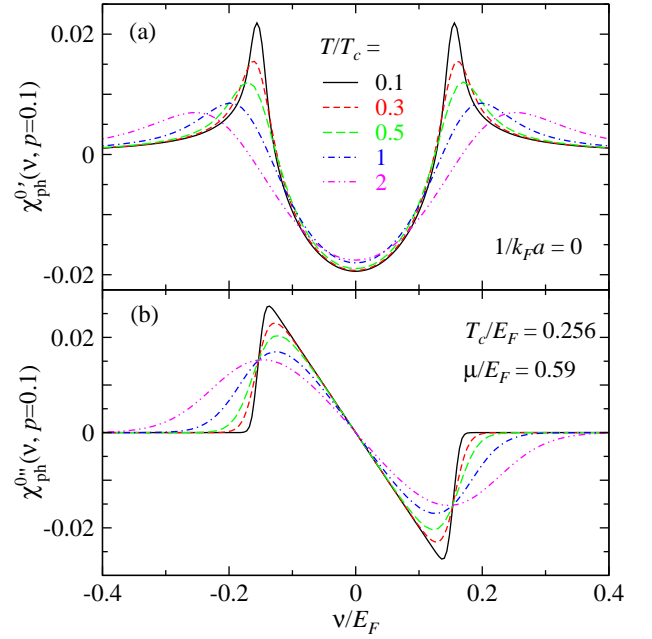


Figure 12. (Color online) The undressed particle-hole susceptibility $\chi_{ph}^{0R}(\nu, p = 0.1)$ for different T (as labeled) at unitarity and momentum $p = 0.1$. As in Fig. 11, we fix $\mu = 0.59$.

result (not shown) demonstrates that the real part presents a double peak structure, with the peaks becoming increasingly broader as T increases. At low T , the location of the peaks are roughly given by $\nu = \pm p k_\mu / m \approx \pm 0.15$ for $\mu = 0.59$ at unitarity. This relation also shows how the $\chi_{ph}^{0R}(\nu, p)$ curves evolve with total momentum p .

Next, we investigate how the particle-hole susceptibility $\chi_{ph}^R(\nu, p)$ evolves with total momentum p in the presence of feedback effect. Shown in Fig. 14 are the curves of the real and imaginary parts for increasing p for a unitary Fermi gas, calculated at T_c . Just as in Fig. 11, the $p = 0$ curve shows a clear gap in the neighborhood of $\nu = 0$ in the imaginary part, $\chi_{ph}''(\nu, p)$. As p increases, this gap gradually disappears, and the upper bound in ν beyond which $\chi_{ph}''(\nu, p)$ vanishes increases towards infinity. At the same time, the peaks in the real part becomes broader and smeared out. From Fig. 14(a), we can see that at $\nu = 0$, the real part slowly increases with p .

The zero frequency value $\chi'_{ph}(0, p)$ is plotted in Fig. 4 in the text as a function of p .

Finally, we show in Fig. 15 the angular average of the on-shell particle-hole susceptibility, $\langle \chi_{ph}(0, p = |\mathbf{k} + \mathbf{k}'|) \rangle$ at $\nu = 0$ as a function of momentum k/k_F , under the condition $k = k'$, calculated at $1/k_F a = 0.5$. The chemical potential is nearly zero, close to the boundary separating fermionic and bosonic regimes. In comparison with the unitary case shown in Fig. 6, we conclude that both dressed and undressed particle-hole susceptibility exhibit stronger temperature and k dependence. Here the small chemical potential determines that the susceptibility is also much smaller. It is worth mentioning that the level 1 average of the undressed particle-hole susceptibility actually shows a much stronger temperature de-

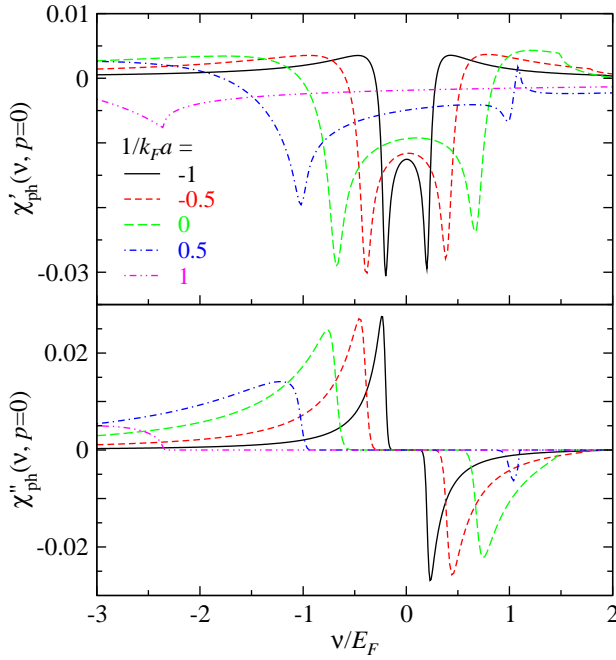


Figure 13. (Color online) The real and imaginary parts of particle-hole susceptibility $\chi_{ph}^R(\nu, 0)$ in the presence of self-energy feedback for various values of $1/k_F a$ from BCS to BEC. The curves are calculated at $0.1T_c$. For each case, the parameters Δ , μ and T_c are calculated using the pairing fluctuation theory without the particle-hole channel effect.

pendence. This is because $1/k_F a$ is very close to the fast shut-off shown in Fig. 7.

-
- [1] D. M. Eagles, Phys. Rev. **186**, 456 (1969).
 - [2] A. J. Leggett, in *Modern Trends in the Theory of Condensed Matter* (Springer-Verlag, Berlin, 1980) pp. 13–27.
 - [3] P. Nozières and S. Schmitt-Rink, J. Low Temp. Phys. **59**, 195 (1985).
 - [4] R. Friedberg and T. D. Lee, Phys. Lett. A **138**, 423 (1989).
 - [5] T. Friedberg and T. D. Lee, Phys. Rev. B **40**, 6745 (1989).
 - [6] J. W. Serene, Phys. Rev. B **40**, 10873 (1989).
 - [7] C. A. R. Sá de Melo, M. Randeria, and J. R. Engelbrecht, Phys. Rev. Lett. **71**, 3202 (1993).
 - [8] M. Randeria, J.-M. Duan, and L.-Y. Shieh, Phys. Rev. Lett. **62**, 981 (1989).
 - [9] L. Belkhir and M. Randeria, Phys. Rev. B **45**, 5087 (1992).
 - [10] M. Randeria, in *Bose Einstein Condensation*, edited by A. Griffin, D. Snoke, and S. Stringari (Cambridge Univ. Press, Cambridge, 1995) pp. 355–92.
 - [11] J. Ranninger and J. M. Robin, Phys. Rev. B **53**, R11961 (1996).
 - [12] R. Micnas and S. Robaszkiewicz, Cond. Matt. Phys. **1**, 89 (1998).
 - [13] R. Haussmann, Z. Phys. B **91**, 291 (1993).
 - [14] O. Tchernyshyov, Phys. Rev. B **56**, 3372 (1997).
 - [15] J. M. Singer, M. H. Pedersen, T. Schneider, H. Beck, and H. G. Matuttis, Phys. Rev. B **54**, 1286 (1996).
 - [16] Y. J. Uemura, Physica C **282-287**, 194 (1997).
 - [17] B. Jankó, J. Maly, and K. Levin, Phys. Rev. B **56**, R11407 (1997).
 - [18] J. Maly, B. Jankó, and K. Levin, Physica C **321**, 113 (1999).
 - [19] J. Maly, B. Jankó, and K. Levin, Phys. Rev. B **59**, 1354 (1999).
 - [20] I. Kosztin, Q. J. Chen, B. Jankó, and K. Levin, Phys. Rev. B **58**, R5936 (1998).
 - [21] Q. J. Chen, I. Kosztin, B. Jankó, and K. Levin, Phys. Rev. Lett. **81**, 4708 (1998).
 - [22] Q. J. Chen, I. Kosztin, B. Jankó, and K. Levin, Phys. Rev. B **59**, 7083 (1999).
 - [23] Q. J. Chen, I. Kosztin, and K. Levin, Phys. Rev. Lett. **85**, 2801 (2000).
 - [24] Q. J. Chen and J. R. Schrieffer, Phys. Rev. B **66**, 014512 (2002).
 - [25] P. Pieri and G. C. Strinati, Phys. Rev. B **61**, 15370 (2000).
 - [26] N. Andrenacci, P. Pieri, and G. C. Strinati, Phys. Rev. B **68**, 144507 (2003).
 - [27] E. V. Gorbar, V. M. Loktev, and S. G. Sharapov, Physica C **257**, 355 (1996); V. P. Gusynin, V. M. Loktev, and S. G. Sharapov, JETP Lett. **65**, 182 (1997); M. Marini, F. Pistolesi, and G. C. Strinati, Eur. Phys. J. B **1**, 151 (1998).
 - [28] J. Quintanilla, B. L. Gyorffy, J. F. Arnett, and J. P. Wallington, Phys. Rev. B **66**, 214526 (2002).
 - [29] Q. J. Chen, J. Stajic, S. N. Tan, and K. Levin, Phys. Rep. **412**, 1 (2005); Q. J. Chen, J. Stajic, and K. Levin, Low Temp. Phys., **32**, 406 (2006), [Fiz. Nizk. Temp. **32**, 538 (2006)].
 - [30] C. A. Regal, C. Ticknor, J. L. Bohn, and D. S. Jin, Nature **424**, 47 (2003).
 - [31] M. Greiner, C. A. Regal, and D. S. Jin, Nature **426**, 537 (2003).
 - [32] C. A. Regal, M. Greiner, and D. S. Jin, Phys. Rev. Lett. **92**, 040403 (2004).
 - [33] S. Jochim *et al.*, Science **302**, 2101 (2003).
 - [34] M. Bartenstein, A. Altmeyer, S. Riedl, S. Jochim, C. Chin, J. H. Denschlag, and R. Grimm, Phys. Rev. Lett. **92**, 120401 (2004).
 - [35] M. Bartenstein, A. Altmeyer, S. Riedl, S. Jochim, C. Chin, J. H.

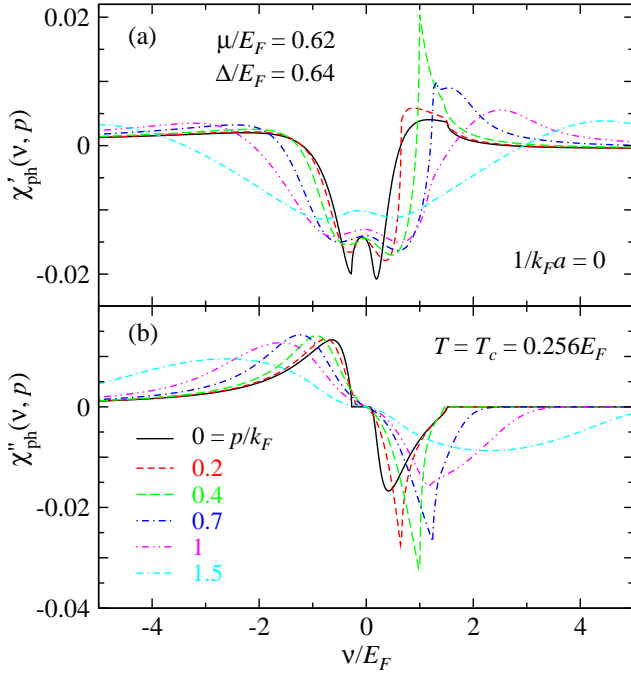


Figure 14. (Color online) The particle-hole pair susceptibility $\chi_{ph}^R(\nu, p)$ at unitarity and at T_c in the presence of self-energy feedback for increasing $p = 0, 0.2, 0.4, 0.7, 1$, and 1.5 . The parameters Δ , μ and T_c are calculated using the pairing fluctuation theory without the particle-hole channel effect. As p increases, the peaks becomes broader and smeared out, and the upper bound in ν beyond which $\chi_{ph}''(\nu, p)$ vanishes increases towards infinity. In addition, the well defined gap at $p = 0$ in $\chi_{ph}''(\nu, p)$ near $\nu = 0$ gradually disappears.

Denschlag, and R. Grimm, Phys. Rev. Lett. **92**, 203201 (2004).
[36] M. W. Zwierlein *et al.*, Phys. Rev. Lett. **91**, 250401 (2003).
[37] M. W. Zwierlein, C. A. Stan, C. H. Schunck, S. M. F. Raupach, A. J. Kerman, and W. Ketterle, Phys. Rev. Lett. **92**, 120403 (2004).
[38] M. W. Zwierlein, J. R. Abo-Shaeer, A. Schirotzek, and W. Ketterle, Nature **435**, 170404 (2005).
[39] J. Kinast, S. L. Hemmer, M. E. Gehm, A. Turlapov, and J. E. Thomas, Phys. Rev. Lett. **92**, 150402 (2004).
[40] J. N. Milstein, S. J. J. M. F. Kokkelmans, and M. J. Holland, Phys. Rev. A **66**, 043604 (2002).
[41] Y. Ohashi and A. Griffin, Phys. Rev. Lett. **89**, 130402 (2002).
[42] A. Griffin and Y. Ohashi, Phys. Rev. A **67**, 063612 (2003).
[43] J. Stajic, J. N. Milstein, Q. J. Chen, M. L. Chiofalo, M. J. Holland, and K. Levin, Phys. Rev. A **69**, 063610 (2004).
[44] A. Perali, P. Pieri, L. Pisani, and G. C. Strinati, Phys. Rev. Lett. **92**, 220404 (2004).
[45] H. Hu, A. Minguzzi, X.-J. Liu, and M. P. Tosi, Phys. Rev. Lett. **93**, 190403 (2004).
[46] H. Heiselberg, Phys. Rev. Lett. **93**, 040402 (2004).
[47] G. M. Falco and H. T. C. Stoof, Phys. Rev. Lett. **92**, 130401 (2004).
[48] T. Bourdel, L. Khaykovich, J. Cubizolles, J. Zhang, F. Chevy, M. Teichmann, L. Tarruell, S. J. Kokkelmans, and C. Salomon, Phys. Rev. Lett. **93**, 050401 (2004).
[49] M. Greiner, C. A. Regal, and D. S. Jin, Phys. Rev. Lett. **94**, 070403 (2005).

[50] Q. J. Chen, C. A. Regal, M. Greiner, D. S. Jin, and K. Levin, Phys. Rev. A **73**, 041601 (2006).
[51] G. B. Partridge, K. E. Strecker, R. I. Kamar, M. W. Jack, and R. G. Hulet, Phys. Rev. Lett. **95**, 020404 (2005).
[52] Q. J. Chen and K. Levin, Phys. Rev. Lett. **95**, 260406 (2005).
[53] Q. J. Chen, J. Stajic, and K. Levin, Phys. Rev. Lett. **95**, 260405 (2005).
[54] H. Hu, X. J. Liu, and P. D. Drummond, Europhys. Lett. **74**, 574 (2006).
[55] E. Taylor, A. Griffin, N. Fukushima, and Y. Ohashi, Phys. Rev. A **74**, 063626 (2006); N. Fukushima, Y. Ohashi, E. Taylor, and A. Griffin, Phys. Rev. A **75**, 033609 (2007).
[56] A. Altmeyer, S. Riedl, C. Kohstall, M. J. Wright, R. Geursen, M. Bartenstein, C. Chin, J. HecherDenschlag, and R. Grimm, Phys. Rev. Lett. **98**, 040401 (2007).
[57] J. Kinast, A. Turlapov, and J. E. Thomas, Phys. Rev. Lett. **94**, 170404 (2005).
[58] M. W. Zwierlein, C. H. Schunck, A. Schirotzek, and W. Ketterle, Nature (London) **442**, 54 (2006).
[59] G. B. Partridge, W. H. Li, Y. A. Liao, R. G. Hulet, M. Haque, and H. T. C. Stoof, Phys. Rev. Lett. **97**, 190407 (2006).
[60] J. R. Schrieffer, *Theory of Superconductivity*, 3rd ed. (Perseus Books, Reading, MA, 1983).
[61] L. P. Gorkov and T. K. Melik-Barkhudarov, Sov. Phys. JETP **13**, 1018 (1961).
[62] N. F. Berk and J. R. Schrieffer, Phys. Rev. Lett. **17**, 433 (1966).
[63] H. Heiselberg, C. J. Pethick, H. Smith, and L. Viverit, Phys. Rev. Lett. **85**, 2418 (2000).
[64] D.-H. Kim, P. Torma, and J.-P. Martikainen, Phys. Rev. Lett. **102**, 245301 (2009).
[65] J.-P. Martikainen, J. J. Kinnunen, P. Torma, and C. J. Pethick, Phys. Rev. Lett. **103**, 260403 (2009).
[66] Z.-Q. Yu, K. Huang, and L. Yin, Phys. Rev. A **79**, 053636 (2009).
[67] A. J. Leggett, Nat. Phys. **2**, 134 (2006).
[68] Q. J. Chen and K. Levin, Phys. Rev. B **78**, 020513(R) (2008).

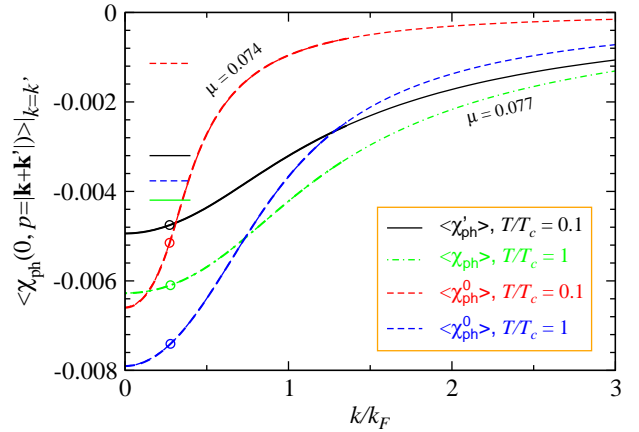


Figure 15. (Color online) Angular average of the on-shell particle-hole susceptibility, $\langle \chi_{ph}(0, p = |\mathbf{k} + \mathbf{k}'|) \rangle_{|\mathbf{k}=\mathbf{k}'}$ at $\nu = 0$ as a function of momentum k/k_F , under the condition $k = k'$, calculated at $1/k_F a = 0.5$. The conventions and legends are the same as in Fig. 6. Here $T_c = 0.226 E_F$ and the chemical potential $\mu/E_F = 0.077$ and 0.074 at T_c and $0.1 T_c$, respectively. Clearly, there are even stronger temperature and k dependencies in both $\langle \chi_{ph}(0, p) \rangle$ and $\langle \chi_{ph}^0(0, p) \rangle$ than the unitary case shown in Fig. 6. The (absolute) values of Level 2 average are substantially smaller than their level 1 counterpart.

- [69] T. Timusk and B. Statt, Rep. Prog. Phys. **62**, 61 (1999).
- [70] R. Damasceli, Z. Hussain, and Z.-X. Shen, Rev. Mod. Phys. **75**, 473 (2003).
- [71] J. Kinast, A. Turlapov, J. E. Thomas, Q. J. Chen, J. Stajic, and K. Levin, Science **307**, 1296 (2005), published online 27 January 2005; doi:10.1126/science.1109220.
- [72] Y. He, Q. J. Chen, and K. Levin, Phys. Rev. A **72**, 011602(R) (2005).
- [73] Q. J. Chen and K. Levin, Phys. Rev. Lett. **102**, 190402 (2009).
- [74] J. T. Stewart, J. P. Gaebler, and D. S. Jin, Nature (London) **454**, 744 (2008).
- [75] J. P. Gaebler, J. T. Stewart, T. E. Drake, D. S. Jin, A. Perali, P. Pieri, and G. C. Strinati, Nat. Phys. **6**, 569 (2010).
- [76] L. P. Kadanoff and P. C. Martin, Phys. Rev. **124**, 670 (1961).
- [77] B. R. Patton, Phys. Rev. Lett. **27**, 1273 (1971).
- [78] Q. J. Chen, *Generalization of BCS theory to short coherence length superconductors: A BCS-Bose-Einstein crossover scenario*, Ph.D. thesis, University of Chicago (2000), (freely accessible in the ProQuest Dissertations & Theses Database online).
- [79] Y. He, C.-C. Chien, Q. J. Chen, and K. Levin, Phys. Rev. B **76**, 224516 (2007).
- [80] The contribution of the particle-hole channel T -matrix appears (as the last diagram) in Fig. 2.2(a) of Ref. 78, but was later dropped in the derivation of the pairing fluctuation theory, which focuses primarily on the pairing phenomena in particle-particle channel. Nevertheless, one can see from this figure that the mixing of G_0 and G' appears in both the particle-particle and particle-hole susceptibilities.
- [81] H. Hu, P. D. Drummond, and X. J. Liu, Nat. Phys. **3**, 469 (2007).
- [82] H. Hu, X.-J. Liu, and P. Drummond, Phys. Rev. A **77**, 061605(R) (2008).
- [83] R. Haussmann, W. Rantner, S. Cerrito, and W. Zwerger, Phys. Rev. A **75**, 023610 (2007).
- [84] S. Floerchinger, M. Scherer, S. Diehl, and C. Wetterich, Phys. Rev. B **78**, 174528 (2008).
- [85] K. B. Gubbels and H. T. C. Stoof, Phys. Rev. Lett. **100**, 140407 (2008).
- [86] E. Burovski, N. Prokof'ev, B. Svistunov, and M. Troyer, Phys. Rev. Lett. **96**, 160402 (2006).
- [87] O. Goulko and M. Wingate, Phys. Rev. A **82**, 053621 (2010).
- [88] V. K. Akkineni, D. M. Ceperley, and N. Trivedi, Phys. Rev. B **76**, 165116 (2007).
- [89] L. Luo, B. Clancy, J. Joseph, J. Kinast, and J. E. Thomas, Phys. Rev. Lett. **98**, 080402 (2007).
- [90] L. Luo and J. E. Thomas, J. Low Temp. Phys. **154**, 1 (2009).
- [91] M. J. H. Ku, A. T. Sommer, L. W. Cheuk, and M. W. Zwierlein, "Revealing the superfluid lambda transition in the universal thermodynamics of a unitary fermi gas," ArXiv:1110.3309.
- [92] R. Combescot, A. Recati, C. Lobo, and F. Chevy, Phys. Rev. Lett. **98**, 180402 (2007).